# Newsletter

nl-iaeg ingeo kring
Stiching IAEG 1990

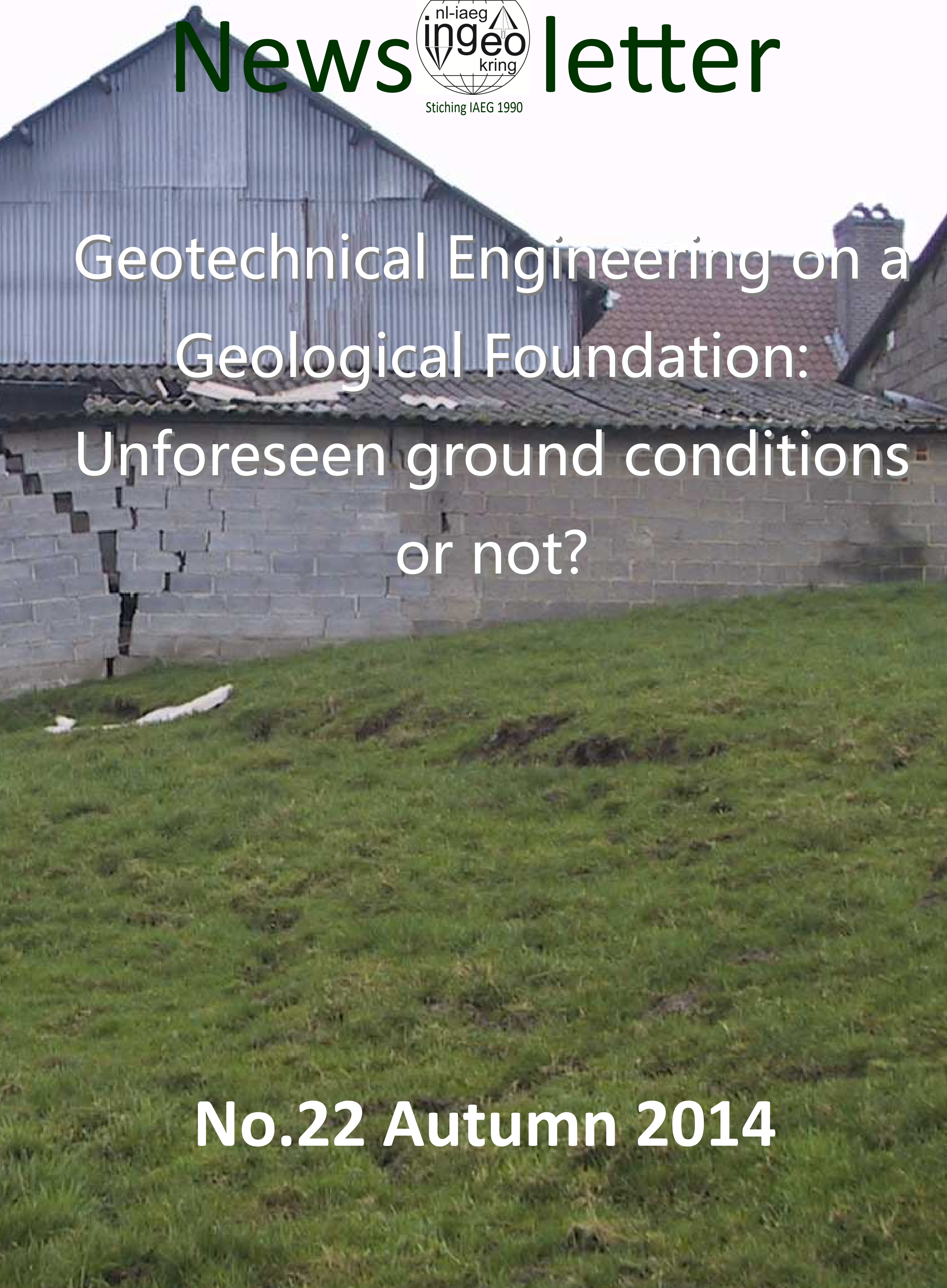

# Geotechnical Engineering on a Geological Foundation: Unforeseen ground conditions or not?

No.22 Autumn 2014

# Colophon

*Ingeokring, founded in 1974, is the Dutch association of engineering geologists. It is the largest section of KNGMG (Royal Geological and Mining Society of The Netherlands). Ingeokring also forms the Netherlands National Group of the International Association for Engineering Geology and the Environment (IAEG).*

*With **over 150 members** working in different organisations, ranging from universities and research institutes to contractors, from consultancy firms to various governmental organizations, Ingeokring plays a vital role in the communication between engineering geologists in The Netherlands.*

*The objective of the Newsletter is to inform members of the Ingeokring and other interested parties about topics related to engineering geology, varying from detailed articles, book reviews and student affairs to announcements of the Ingeokring and current developments in the field of engineering geology. The Newsletter wants to make engineering geology better known by improving the understanding of the different aspects of engineering geology.*



**All correspondence should be addressed to:**

Ingeokring Newsletter

Delft University of Technology. Faculty of Civil Engineering and Geosciences, Geo-Engineering Section

P.O. Box 5048

2600 GA  Delft

E-mail: info@ingeokring.nl

**Subscription to the Newsletter**

Each member of the Ingeokring receives at least once a year a new edition of the Newsletter. Membership fee for the Ingeokring is **€18; student membership fee is €9.** Other membership alternatives can be found at:

http://www.ingeokring.nl/pages/membership.php

**Issue**

*Geotechnical Engineering on a Geological Foundation: Unforeseen ground conditions or not?*

Winter 2014-2015 (**150** copies)

**Cover photo**

Belgian farm house located on a hill damaged by slow slope movement, Université de Liège, Robrecht Schmitz, 2002

**Guidelines for authors of Newsletter articles and information about advertising in the Newsletter can be found at the inside of the back cover.**

**ISSN 1384-1351**

# Table of contents

# Newsletter editorial developments

***Michiel Maurenbrecher***

Our principal editor, Eric Schouten, resigned leaving a gaping void and a position vacant difficult to emulate. He managed to bring the newsletter to such a high standard usually only achieved by journals having much larger editorial staff of which many are professionally employed to cover many of the different aspects of producing the journal: Articles (usually procured by the editor or submitted by members for publishing), advertising for helping offset the costs, checking the texts for grammar, spelling, comprehension and scientific/professional content and, possibly the most difficult aspect, is to arrange the layout of the manuscripts into an attractive publication. There was an editorial committee for the IngeoKring newsletter but it tended to form a mentor group for Eric. The other facets of the editorial committee he tended to combine. I can fully understand this: often it involves spending much time delegating the various chores to the board members where-as this process can take up more time than just performing all the journal facets oneself. I was much in that situation when running the Netherlands association of members of the Institution of Civil Engineers (UK) as their chairman ending up with the portfolios of finances, events, contacts (KIvI-ICE), and more informally issuing an annual newsletter, posting it each year with the Christmas mail with the heading 'Prospect 2003 to 2011); by 2011 I handed over the Chairmanship and other portfolios to a new chairman and committee, remaining with one item: liaison KIvI-ICE. Though over the years I have made contributions to the Newsletter in the shape of articles, columns and papers I avoided the financial and production aspects of the Newsletter so with Eric vacating his position on the newsletter I became, de facto, an interim editor to hopefully offer some continuity in newsletter production. Since 1976 these have been issued on an irregular basis so at various periods the issues appeared monthly, quarterly, yearly and a few times bi-annually! The issues have also varied style from initially a typewriter photocopied duplication followed by personal computer word processed articles printed out (the first issue on matrix printers) followed by print-out duplicated by photocopies. Quality varied depending on the printer and the photocopier ribbon or ink levels. Graphic material has improved over the years but so has its attended complication as a drawing produced by one software may not keep its 'integrity' when used by another. At the start colour was not an option so that photographs had to be photocopied using a raster overlay and grey shades conversion from colours was left to the photocopier. Today's whole issues can be printed direct from the file using the word processor print instructions onto a printer which resembles (and also function as) a colour photocopier. This activity is often delegated, at cost, to a printing company who further add a cover and bind the issues. This stage can be avoided and has become an option to subscribers at reduced subscription by offering electronic issues, saving on postage, paper and printing and considerable time and effort on the part of the editorial board. This makes sense to those producing the newsletter on a voluntary basis in their spare time. Issues can even be produced in an initial 'draft' version so that having to check for 4errors in text: content, grammar, spelling and graphics, of which content can be left to the reader who can return an errata list to the editor so that changes can be made on a more-or-less continual basis to the issue with hopefully fewer modifications with time . ..

I was asked to provide the copy about IngeoKring activity for the first edition of the 'monthly' newsletter as, IngeoKring's new President , Robrecht Schmitz observed that I was making notes " in that 'pocket notebook of yours'. You must have some good notes on a joint IngeoKring (of the KNGMG and the Geotechnical Section of KIvI-NIRIA held in 7 November 2013, an IngeoKring field visit to Nijmegen and a combined KNGMG 'kringen' field meeting for the Maasvlakte 2 Rotterdam Harbour extension into the North Sea…etc. etc.". He should have said "In that orange A6 booklet with a football depicted as a page marker; a purchase made after the last World Cup in 2010 (they sell for half price at Schiphol). So an attempt has been made to try and unscramble the scribbles in a this notebook which fortuitously contain the activities from 2013 to date. (Also events not to do with IngeoKring but certainly provided article material for the newsletter, i.e. a trip to Scotland's Firth of Clyde (un-intentional all the way from Glasgow to Troon) a circular rail trip from the Hague via Brussels to Luxembourg, returning via Liege and Maastricht. Meeting of the Institution of Civil Engineers members hosted by the Luxembourg ICE Association with a presentation by Professor Robert Mair (Geotechnical Engineering, Cambridge University) and an ELAC (European Local Associations Conference) again hosted by LuxICE plus a travelogue on a more-or-less circular railway journey to Luxembourg and a railway journey to and from Maastricht with an overnight stay at a boutique hotel in the old centre to meet Robert

Broatch (FranceICE) and his wife Joelle from Paris. I took them to visit the Natural History Museum nearby the hotel to show them the cast of the fossil bones of the Mosasaurus, of which the original skeleton Napoleon had requisitioned for France, hinting that we (the Netherlands) would like it returned. To make distinctions between my social and professional activities increasingly overlap so that even a vacation as guest to a wedding in the Cote d'Azur resort of St. Jean Cap Ferrat with its backdrop of maritime Alpinism one could not easily lie on a beach and block out the geology. One of the guests also happens to be a geologist so the rock of Cap Ferrat became more than just a jumble of jointed limestone.

# Symposium: Geotechnical Engineering on a Geological Foundation: Unforeseen ground conditions or not?

***Michiel Maurenbrecher***

November 21, 2013 the yearly Ingeokring symposium was organised at Delft University of Technology, entitled: Geotechnical Engineering on a Geological Foundation: Unforeseen ground conditions or not?

Five invited speakers provided excellent examples demonstrating the importance of engineering geology for risk assessment in geotechnical engineering:

- Joost van der Schrier (Royal Haskoning DHV, retiring Chairman IngeoKring) "Understanding geotechnical risk from geological perspective"
- Prof. Dr. Christian Schroeder (Université Libre de Bruxelles) "Geological maps help anticipating problems…"
- Dr. Ulrich Polum and Charlotte Krawczyk (EAEG) "Geophysics to support Geotechnics"
- Marc Van Den Broeck (Department Manager RMPE, DEME, Belgium)
- Arjan Venmans (Deltares) "Application of the Geo-Impuls toolkit to road construction on soft soil: putting numbers on geology"

On the following pages I summarize the highlights of the symposium. Some of the presenters during the symposium provided extended abstract and articles related to their talk, which are presented later in this issue. At the end of the symposium the "Prof. Price prize" and the "Best thesis award" were awarded.

Joost van der Schrier (Royal Haskoning DHV, retiring Chairman IngeoKring) "Understanding geotechnical risk from geological perspective" The only example I know on risk analysis is from my student times for my first degree in civil engineering from a recording of Gerard Hoffnung reading out in 1958 at the Oxford (students) Union a letter purportedly, he says, published in a 'recent bulletin of Civil Engineering Contractors ' written by a hospitalised bricklayer requesting sick-leave explaining the reason for his misfortune as a result of a hurricane causing bricks to be blown from a stack unto the ground and the bricklayer's effort to retrieve the fallen bricks by hoisting them by several

*Figure 1: Robrecht Schmitz thanking the speakers from left to right Christian Schroeder, Ulrich Polum, Arjan Venmans, Mark Van Den Broeck and Joost van der Schrier*

barrel-loads using a secured beam, a pulley and a rope. Strangely the last barrel load he found that there were too many bricks so he went down to lower the hoisted barrel-load back down when the change in procedure went wrong… The whole episode is a case history in risk analysis and could have been avoided saving cost and injury. The Oxford students do not seem to take the letter seriously despite that Oxford University has a civil engineering department. (Its on YouTube,). Risk was then equated to safety. Safety is to ensure prevention of injury; this is of paramount importance but "risk" can involve lots more and is difficult to quantify.
Such an event would not have cost much. Today there would be litigation for bad practice and huge damages. Joost introduced his presentation by quoting Fred Baines, recently President of IAEG saying that if proper risk analyses would be done up to $ 1 billion would be saved worldwide. The ground is especially a civil engineering risk area, even if they are foreseen. Not only the ground structure but also the project management structure can be a risk: layer 1: the office, layer 2: the client then 3. Job, 4. Place of work, 5. Pre-finances, 6. Geological environment, and 7, the team.
A few well known engineering geologists and geotechnical engineers were referred to: Glossop: the natural environment and the purpose of building, Fookes: understand the morphology besides just geology; if you do not know what you are looking for you will not find anything of value, by communicating and sharing knowledge we can only go forward. Brunsden giving the 5th Glossop lecture (main annual lecture of the Engineering Group of the Geological Society) stated to link morphology between existing (& previous) morphologies indicates & reflects what is beneath. For the Netherlands by using Google one finds such links levees/ hydraulics of velocities river flow) with archaeological finds in the higher areas of sand banks (link: RGD-Deltares.
I should have contributed to the discussion by adding to the van der Schrier- Baines introduction by stating if proper risk analyses was done up to another $1 billion in losses could be awarded for claimants with appropriate tailored insurance cover, for example, damage to ones property as a result of vibrations: man or naturally induced.
Next Robrecht Schmitz took over as new Chairman of IngeoKring and promptly announced a forthcoming event for June 2014 at Hambach in the upper-Rur valley in the Rheinland schieffer gerbergte, the extension of the Ardennes highly folded Devonian rock into Germany (it exits as the Roer (Dutch spelling) at Roermond into the Maas) on connecting what we see from Geological maps and rock mechanics and what we see in the field excursion with introductory afternoon with presentations and guide-lines with partners and kids.

Prof. Dr. Christian Schroeder (Ecole Polytechnique de Bruxelles & Université Libre de Bruxelles; prviously Université de Liege) "Geological maps help anticipating problems…" Geology maps traditionally show the chrono-statigraphy but newer maps increasingly show the litho-stratigraphy. Possibly I should have asked Prof. Schroeder a question: "is not stratigraphy the classification of geological layers according to age?" because modern geology maps show the "litho-stratigraphy" . That means they would be much more useful to engineering geologists (and geotechnical engineers) as they then show the soil or rock type. Dutch maps go a step further to indicate the lithology-profiles within a particular stratigraphic layer and indicating thereby present and previous geomorphology. . But Christian would like to show on maps or overlays hazard zones or zones 'prone to hazards' or even zones where hazards have resulted in appreciable litigation because of insufficient site investigation. Hazards can be defined from the litho-stratigraphy as, for example, the combination of sand overlying clay are prone to landslides if excavations are made to obtain the clay (say for brick-making). The contact zone between young flood plain sediments and older valley slopes may indicate ongoing slope instability just as a feature but more so if the lithology is given as talus or similar material (i.e. lithology in combination with a relatively young geological age: Quaternary, Holocene or even Anthropocene) Profiles of sand and calcareous sandstone cause subsidence problems to the civil engineering building of the Université Libre because karst voids were created in the sandstone as a result of leaching of the calcareous cementation. The Frasnien stratigraphic layer has predominantly limestone lithology. Karst voids on maps are shown as a circle with a dot in the in middle indicating a "losing stream" presumable a stream draining into a karst feature such as a cave entrance or swallow hole. To determine if there are swallow hole features a grid of dynamic penetrometer tests was recommended.
Appropriately following Prof. Christian Schroeder's talk was Dr. Ulrich Polum (presentation co-author Charlotte Krawczyk (from the Leibnitz Inst. Applied Geophysics) on "Geophysics to support Geotechnics". Dr. Polum is chairman EAEG: ( European Ass. Engineering Geophysics) . Hopefully he would make suggestions of using geophysics to locate karst in the subsurface since he said by way of introduction that the trend in engineering geophysics was to look increasingly in more detail (high resolution) to the shallower subsurface though many techniques do not apply such as magnetics and satellite gravity surveys. The most effective method is geo-radar but it does require skill of operation, more processing skills to increase resolution and restricted in delivering the many parameters requested by geotechnical engi-

neers for their modelling and analyses. One example is the shear modulus G associated with stiffness: Stiffness determined by laboratory tests on soil or rock samples can differ markedly from that derived from seismic velocity measurements associated with the differences in deformation and duration of deformation loading. Despite this seismic surveys can show aquifer boundaries (from a survey done in Hannover). In other instances, probably inappropriate, was to try and investigate earthquakes in an expensive neighbourhood in Hamburg. The investigation was hampered by the subsurface infrastructure of cables, water, sewer and gas mains. At Trondheim, Norway they obtained $G_0$ which gave a good comparison with the CPTU (Piezo-Cone Penetration Test). As the Dutch colloquialism asks: can one compare apples with pears? The comparison fortuitous as one is comparing seismic small strains with CPTU much large strains. And an answer to detect karst features? It did not arise so I suggest sticking to the dynamic penetration tests and have lots of geophones recording the various seismic wave travel times produced by this test and process the whole lot using a Cray-computer: who knows one may get a high revolutionary picture of the subsurface. Let's call it 3-D tomography.

Marc Van Den Broeck (Department Manager RMPE, DEME, Belgium) was the only speaker who did not have a title for his presentation in the flyer sent round by the IngeoKring urging us to attend the symposium. I have in my notebook written "Evolution of Flemish Marine Engineering" and a profound motto "Our …. Interesting beyond failure". From the previous speaker I would have liked to have heard about the evolution of marine geophysics which over the last fifty years has produced stunning results. Since the theme of the conference was "Geotechnical Engineering on a Geological Foundation UNFORESEEN GROUND CONDITIONS OR NOT" one looked forward to Marc to possibly the Belgians for increased sophistication in marine site investigation. Much of the DEME activities are based on the Flemish market Jan de Nul, Dredging International, Scaldis Geosea (windmills) SSE (?) (involved Panama Canal new locks -410m long in basalt rock- is based on the biggest lock at Antwerpen). The remaining involvement for Dredging International is to dredge 1 m sea bed along a 250m wide channel width at the Pacific entrance. Research is done on shore protection as well as quarry sources for rip-rap. Within Benelux DEME are becoming more active as a result of EU contractual (tendering) regulations. The RMPE section Geology and Geotechnical input is obtained through their network of experts from Belgian institutes, the names of Raedeschelde, van Impe, Maertens, van den Berge, Halleux and Goedhals were mentioned. (All the names are familiar and contemporary except the last – I assume, because the name Goedhals I associate with the Panama Canal: He was the US Corp of Engineers General who managed the completion of the canal in 1905. He is descended from a Belgian emigrant to the USA! Subsidence due to karst requires innovative research so when dealing with this at a tender stage for a jetty in Australia on large diameter piles DEME submit alternatives even if the costs may be higher which they won in competition with a combined tender from Bos Kalis and van Oord. Offshore wind farms also require increasingly innovative solutions especially that the diameters of the blades are exceeding 150m. Underwater turbines also need specialist design approach as currents of 8 m/s must be coped with. Though most design and construction has succeeded some still have to be resolved such as proposals for the Farnbelt tunnel in glacial tills, Denmark.
Marc's main contribution to the presentation is a criticism and a plea (I assume he did say more than the activities of DEME-RMPE and what the actual innovations were… though I read recently the Jan de Nul (DEME) have large claims for unforeseen costs against the Panama Canal Authority) was that many geotechnical models (I found this from my own experience too) that the academics produce models containing up to 40 odd parameters of which 90% cannot be measured. Probably he must be referring to those models in the no-mans land of soil mechanics and hydraulics involving sediment transport, sedimentation and consolidation with a few erosion cycles to complicate the issue. It does not end there as biological influences cause havoc with the classical soil mechanics consolidation theory as creatures (worms, larvae) bury, consume and expel sediments and even smaller ones (algae) act as catalysts causing cementation so that the whole process creates a large population of parameters for a marine hydraulics-geotechnical model which for engineering geologists will be more difficult to understand as quantum theory is for ________________________________. (Fill in what you think is most appropriate).

Last but not least presenter was Arjan Venmans (Deltares) "Application of the Geo-Impuls toolkit to road construction on soft soil: putting numbers on geology. I must be forgiven if I got the numbers wrong but possibly times have changed and anything less than €100 m is not worth a mention; hence the Geo-impulse involve figures of €150 m to €300 m and €1 m/year. I presume on figure quotes its worth another the amount of potential expenses from failures, over-design saved and the last more moderate figure is the yearly running and maintenance of the main DINO facility central to the GeoImpuls project. Before trying to decipher my notes I decided to visit the DINO loket at which as with many websites I visit I am confronted with having to make impossible decisions with regard to up loads together with dire warnings that they may contain infectious viruses which could spell death to computer. This time I needed an Adobe Flash-player as my iPad does not have it. I tried then my desk computer and I did get into the system but it seemed to go quite slow. Probably one had to get used to interacting with DINO. I looked at two locations: my house in the Hague and a site in Pijnacker which I am investigating which I thought would be 'nice' to show for my presentation at the IAEG in two weeks' time in Turin. The downloads were not very satisfying but that was just very preliminary. Arjan had in his title how to use the Geo Impuls toolkit for road construction to which he added by asking 'How do we achieve and produce a reliable subsurface model to geotechnical profile; from a 'noisy model' to a geotechnical profile. The website portal for this would be available by January 2014. Presumably before that time Geoimpulse was still being built up to collect information, identify, analyse, quantify, evaluate and transfer risk. The DINO loket database has a voxel (3D volume representing one pixel) of 100m x 100m 1 m thick resolution and for the Netherlands (DINO=Digitaale Informatiesysteem van de Nederlandse Ondergrond) containing now up to 450000 CPTs. Maps of reliability and bandwidth can be produced. Help! That is all I have from my little 2010 WK orange notebook. When I flipped the page of my note book I make jottings of the next event a day later to drive myself without TomTom to a location I looked up on the inferior (to Google); iPad Maps. The announcement was forwarded to me by Robrecht as he hoped someone would be there from the IngeoKring. I drove there though I had recently managed as a 'pensionado' to travel by public transport using an OV card allowing me to have a 40% reduction on travel fares, a few weeks earlier I went to Sluiskil tunnel visit at the southern end of Terneuzen by public transport using OV9292

Before retiring to the traditional "borrel" in the geoengineering lobby, Robrecht Schmitz announced the winner of best thesis for 2013, the Prof. David Price award, was Esther Rosenbrand (TU Delft) on "Investigation into quantitative visualization of suffusion".

# Geological maps help anticipating problems in geotechnical engineering as case studies from Belgium demonstrate

***Prof. Dr. ir. Christian Schroeder*** (*Université Libre de Bruxelles, Bruxelles, CES Consult sprl, Namur CES-Consult@skynet.be)*
***Dr. ir. EurGeol. Robrecht Schmitz*** (*CEng, Int. PE (UK), CGeol, CEnv, UK Registered Ground Engineering Adviser; Belgian-Luxembourgian Union of Geologists, Belgium and Ingeokring, the Netherlands; robrecht.schmitz@alumni.ulg.ac.be)*

**Introduction**

We will show in this contribution, that conceptual engineering geological models for a site can be made on the basis of a geological map (its interpretation), a book describing the general geology of the region and knowledge of the local history. Based on three case studies we show how such conceptual models can developed and how these can be used to anticipate problems in geotechnical engineering. A short paragraph describing the maps available in Belgium will precede the three case histories. For the case histories it is important to know that Belgium has a sea climate with an average rainfall of 850 mm/year (on average 200 days with rain per year).

**Geological maps in Belgium**

The following maps are available in Belgium:
1) The (chronostratigraphic) geological maps at a 1:40,000 scale published between 1890-1919. They cover the entire surface area of Belgium (except for the terrains added to Belgium in 1920). Most of these maps are more than 100 years old. This creates problems in identifying the position on the map because fortifications have been dismantled, bridges have been removed or built, villages have expanded etc. Additional complications arise from the renaming of stages and the redefinition of boundaries of stages since the 19th and early 20th century (examples have been given by Schmitz and Schroeder 2004).
2) Since the regionalisation of Belgium in the 1990s, the Walloon region started re-mapping (lithostratigraphic maps) the territory digitally on a scale 1:25,000. The state of advance can be followed at Wal (2013).
3) Information about the geology in Flanders can be found at DOV (2014).
4) A project to map Belgium geotechnically started with great enthusiasm in the 1970s. These maps show the thickness of the overburden, the composition of the overburden (grainsize distribution, Atterberg limits), the composition of the rock mass (rock mass rating, RQD etc.). These maps have been composed by the "Institut Géotechnique de l'État", with the contribution of many members of the engineering-geology department of the Université de Liège. At this department the students familiarise with these maps during practical exercises and projects. In this way they learn to appreciate the value of such maps. These maps are highly valued by the construction industry. Unfortunately, the production of these maps ceased before the Belgium territory was covered entirely.

For our three case studies (figure 1) we will use the maps at a 1:40,000 scale because they are available for the entire country and these maps were available at the time when the infrastructure that we will analyse in detail was designed and built and the interaction between the geology and the construction activities occurred.

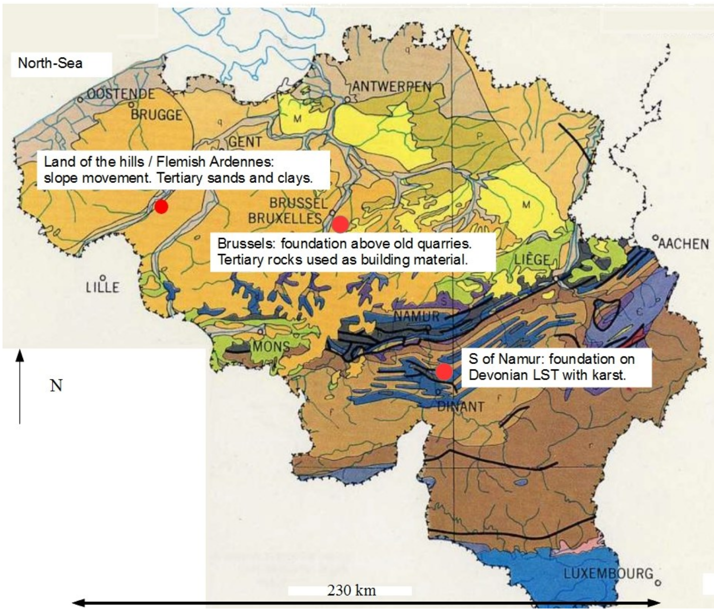


Figure 1. Geological map of Belgium (original scale 1:2,000000, source: Belgian Geological Survey) showing the location of the three case studies discussed in this publication. From the south-east to the north-west formations of Mesozoic (blue), Palaeozoic (brown & purple), Mesozoic (green), Tertiary and Quaternary (both yellow) are encountered. LST: limestone; S: south.

### Case 1: Land of the hills / Flemish Ardennes. Failure of roads and housing caused by slope movement.

*Introduction*

The projects related to this case study are of a small scale (housing and road construction). Failure often occurred after construction. The reason for failure in these cases is predominantly related to slope movement. Examples of such failures are given in figure 2. The budget for engineering-geological site investigations for such small scale infrastructure projects is often low or non-existent. Exhaustive ground characterisation is, except in specific cases, not required by law. What could have been anticipated on the basis of the geological map? An extract of the geological map has been given in figure 3.

*The conceptual engineering-geological model and the geological map on which it is based*

The geological map (figure 3) shows that formations consist of different Eocene clay and sand deposits. The lithologies are predominantly not cemented. Only the youngest layer on the top is cemented, more or less protecting the layers below against erosion. Topographic details and the boundary between the formations show that the layers are oriented horizontally – sub horizontally. In the valley the larger rivers can be found, draining towards the north-east.

On the basis of the geological map the following concept model can be made (figure 4).


Figure 2. Examples of failures caused by slope movement in the Land of the hills / Flemish Ardennes. A: Local road damaged by slow slope movement. B: Fissures in a pasture caused by slope movement (reproduced with permission of Vanhulle, 2005). C: Farm house located on a hill damaged by slow slope movement analysed by the authors in 2002.

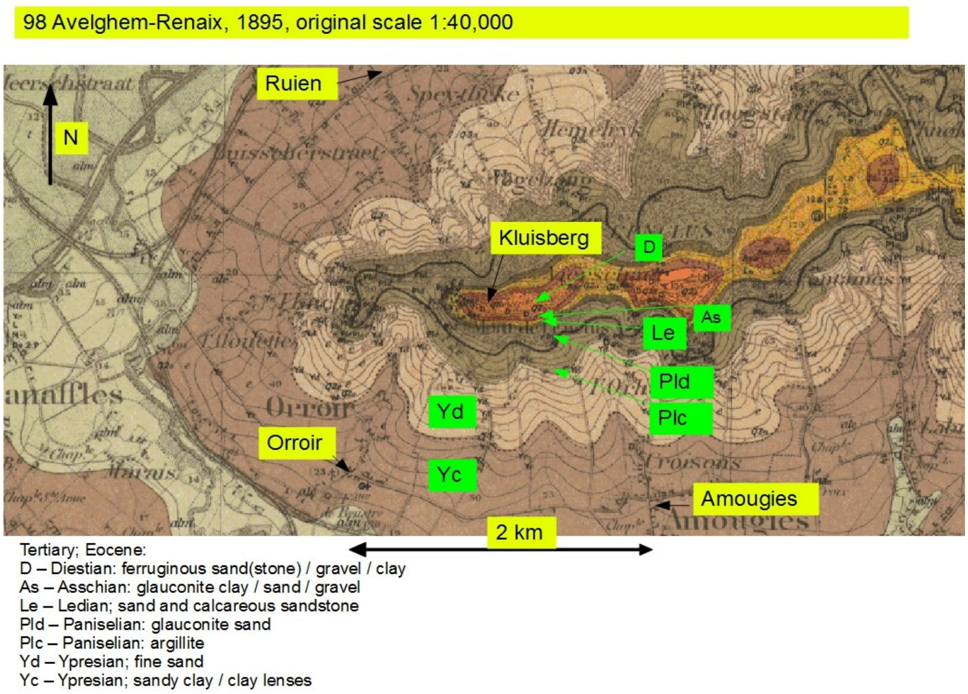


Figure 3. Geological map focussing on the Flemish Ardennes / Land of the hills (here: Kluisberg / Mont de l'Enclus on the border between East-Flanders and Hainaut).

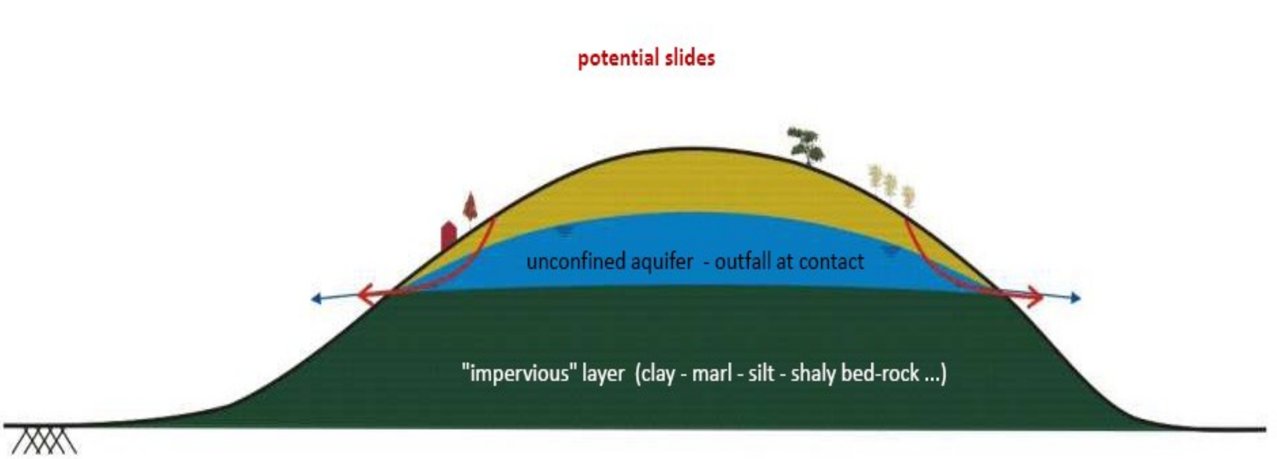


Figure 4. Conceptual engineering-geological model of the terrain on the basis of the geological map.

*Risks identified on the basis of the conceptual engineering-geological model*

The conceptual model includes the following key elements:

The hills are made of soils (in contrast to rock).

Rain water eventually drains towards the larger rivers located in the valleys.

Rain water can infiltrate sandy surface layers and create an unconfined aquifer. Impermeable clay layers form the basis of the aquifer. Water drains from this aquifer at the interface between the impermeable layer, the more permeable sand layer and the slope of the hill.

If the level of the water table increases, with a certain time lag, after periods with high rainfall, the quantity of water draining from the slopes will increase.

Depending on the amount of water and the exact composition of the materials on which the water at the surface of the hill flows, the predicted failure modes are:

**1**) erosion features such as erosion channels (this is a possible risk, depending on the amount of water, the gradient and the exact composition of the hill slope material).

**2**) degradation of the strength of mudrocks. The presence of large amounts of water will certainly weaken claystones, eventually turning these weak rocks into mud (thereby reversing the process of consolidation).

**3**) reduction of the effective stresses and thereby the strength of the materials on the slope.

These risks do not have temporary but a perpetual character.

*What kind of failure does occur?*

In the Walloon Region the region described above is known as the land of the hills (Pays des Collines). In the Flemish Region the region is called the Flemish Ardennes (Vlaamse Ardennen). From a geological (not geographical) point of view the hills are no hills and there is no direct connection to the Ardennes located further farther east. The sand and clay constituting the hills are of Tertiary age. The hills are in fact remnants of a plateau (*getuigenheuvels*, comparable to *Inselbergs*) that have resisted erosion until now. This erosions continuous however. At present conditions the hills are located well above the large rivers draining towards the North-Sea and the hills are subjected to large amounts of rain per year.This causes slope stability problems in many places on theses hills (e.g. Ost et al. 2003 and Eeckhout et al. 2005). This is related to the degradation of the strength of mudrocks and the reduction of effective stresses (points 2 and 3 mentioned above). Erosion feature as described under point 1 does not cause major damage.

*What is the value of the information contained in the geological map?*

If the conceptual model on the basis of the geological map is compared to what happens in this region (figure 2 and Ost et al. 2003 and Eeckhout et al. 2005) two of the three predicted failure modes described above actually occur. Slope movement can be expected on those hills having a steeper incline that the stable angle of the material weakened by water. The stable angle is unfortunately very low (depending on the exact properties of the material) causing many slope stability issues. This example shows that even a geological map from the 19$^{th}$ century is on its own (i.e. without other data) a valuable tool to create good conceptual engineering geological models. These can be used to predict risks related to infrastructure development in the 21$^{st}$ century correctly. A short overview of the geological history of the area has been published by RVLA (2014). Information about the landslides can be found on LNE (2014).

*Table 1. Description of the formations (stages) identified located underneath the construction site of Solbosch campus (case study 2) on the basis of the geological map.*

| Erathem/ Era | Series/ Epoch | Stage/ Age | | Old name | Rock properties I | Rock properties II |
|---|---|---|---|---|---|---|
| Cainozoic | Eocene | Lute-tian | Middel and Upper | Ledian | Exploited since the middle ages in many quarries between the river Scheldt and the river Dyle [a] (Brussels is located in between these rivers). | Calcaire gréseux, sandy limestone [a]. |
| | | Lute-tian | Lower | Brusselian | Pierre de Gobertange. Exploited since hundreds of years in the environs de Jordoigne (30 km of Brussels). Used for the construction of prestigious buildings.(e.g. in Brussels) for a long time . Workability: excellent. Very good mechanical properties to construct e.g. cornices [b]. To he present day the rock is mined in Jordoigne [c]. | Whitish – yellow-grey rock, non oriented grains < 1mm, soft, porous or with alternating fine lamination disturbed by bioturbation [a]. Calcaire gréseux, sandy limestone [a, b, c]. |

[a] Boulvain (2013); [b] PMW (2002); [c] PMW (2012).

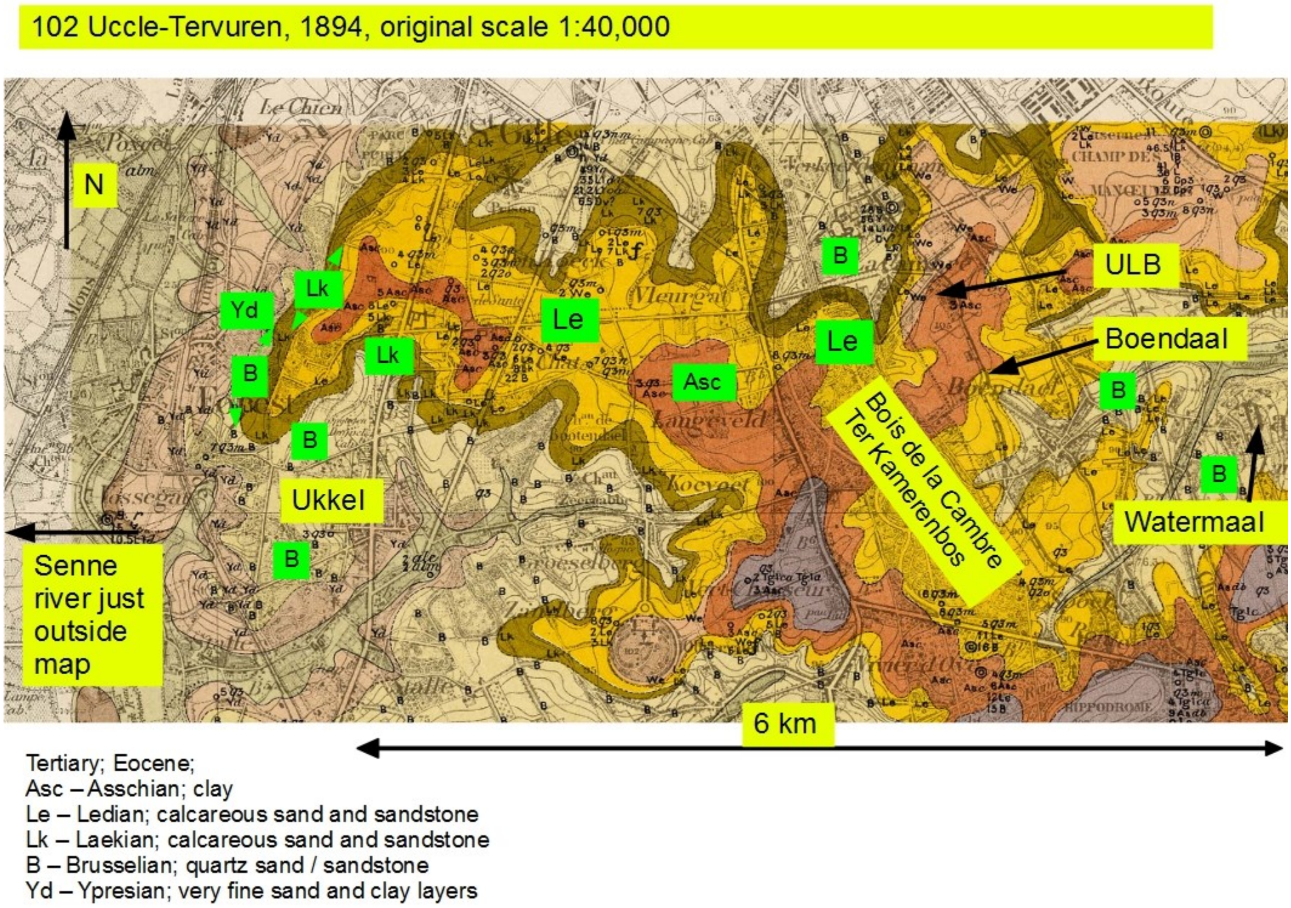


*Figure 5. Geological map of the Solboch region in SE-Brussels.ULB: Université Libre de Bruxelles.*

**Case 2: Foundation above former quarries in Brussels**

*Introduction*

The Université Libre de Bruxelles (ULB), founded in 1834 as counterpart to the three state universities (at that time: Gent, Leuven and Liège) and a catholic university founded in Mechelen, was originally located in the city centre of Brussels. In the 1920s an ULB campus was created in the SE corner of Brussels in an area called Solbosch. On this campus construction of a four-storey building for the civil engineering faculty started in 1953.

*The conceptual engineering-geological model and the geological map on which it is based*

The map shows (figure 5) that the geological stages and the contact between the different stages follow the isolines of equal altitude. On the top there is a quaternary and Eocene soil cover under which rocks of the Ledian stage can be expected. Underneath the Ledian stage rocks, the Brusselian stage rocks can be found. Rocks of this stage crop out in the flanks of the valley of the river Senne, west of the Solbosch campus (Boulvain 2013). On the basis of the geological map a cross section can be drawn. Figure 6 shows a reproduced cross section by Mr Carl Camerman (1885-1958; rock mechanics specialist (PMW 2002)). An overview of the the old stage names used in the map and the new names has been given in table 1. In this table additional background information about the lithologies has been presented.

The geological map reveals that the Quaternary cover did indeed overlay competent rock. This information has to be coupled to other geological and cultural-historical information to produce a useful conceptual engineering-geological model. Since the middle ages till present Brussels has been a large city. In previous centuries natural stone and bricks were the dominant building materials as historic buildings demonstrate. Dreesen and Dussar (2004) show that many different sources of stone were excavated in the vicinity of Brussels. Interesting for the campus construction site is that two different types of Eocene sandstone/sandy limestone were extracted from a region starting in the south-east corner of Brussels and extending further into the hinterland towards the SE. At present excellent building stone is still extracted from formations of Lutetian ages in Gobertange (PMW 2012) south-east of Brussels.

*Risks identified on the basis of the conceptual engineering-geological model*

Just on the basis of these easily, non-exhaustive, available literature sources (a geological map, a handbook that discusses the general geology of the region, a brochure from local producers of natural stones) combined with the information one can obtain from a city walk (looking at the scale of the city, estimating its former size and looking at historic buildings) the conceptual engineering -geological model should include the risk of encountering former sites of stone extraction (whether backfilled or void) (figure 6).

*What kind of failure did occur?*

The constructors expected beneath the soil cover a soft but suitable rock for founding a large multi-story building. Site investigation consisted of cone penetration tests (CPT) to determine the depth and properties of the cover and to prove the presence of competent bedrock. Only

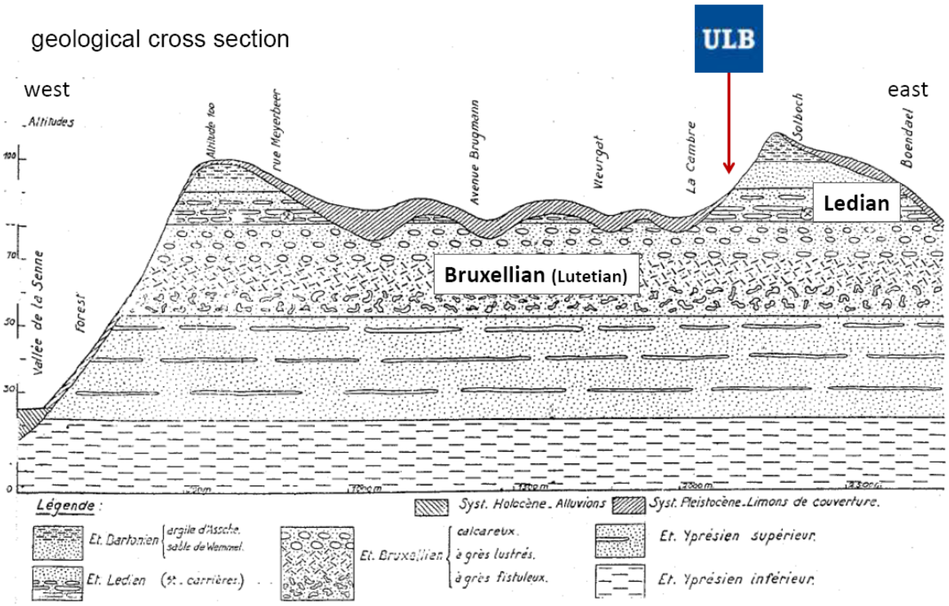


*Figure 6. The conceptual (“actual”) engineering-geological model of the terrain made by Camerman 1955. ULB: Université Libre de Bruxelles.*

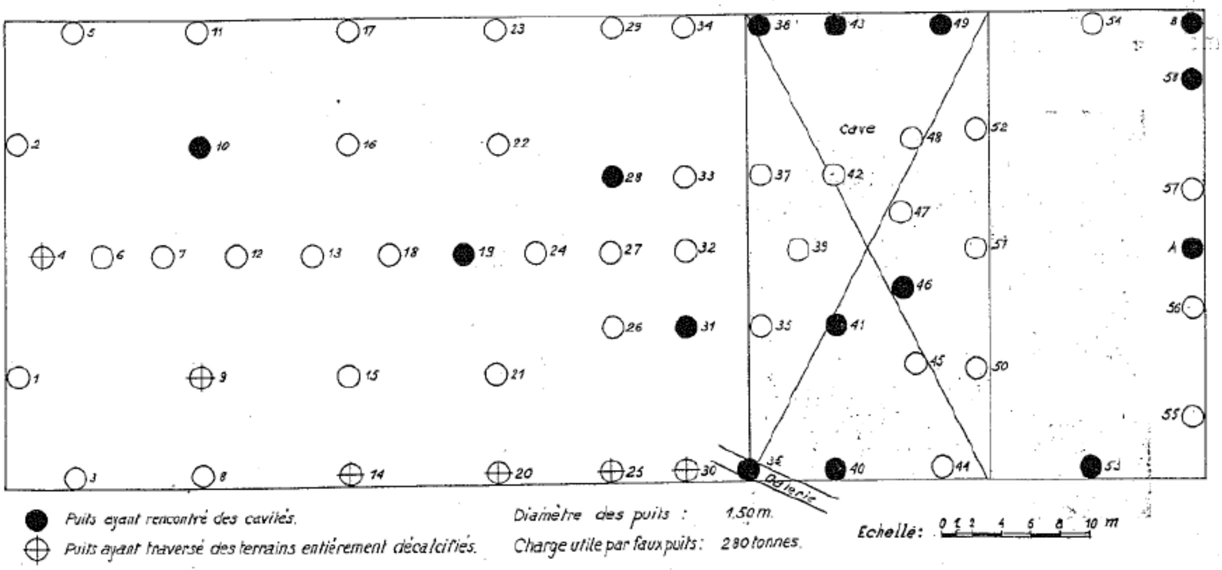


*Figure 7. Location of 59 piles in the adapted foundation design. Black holes indicate where voids were encountered. Holes with crosses show were decalcsified sandstone was encountered during the preparatory work for the 59 piles.*

during construction "shafts" were found that opened into large underground open workings, devoid of rocks, soils or other infill. These excavations were part of an extensive network of forgotten underground quarries. The rock was used as construction material in Brussels and extensively mined.

More CPTs were performed. Where they indicated near 0 MPa resistance,, the constructors decided to change the design and to base the foundation on 59 piles. Large circular holes were excavated and filled with concrete in order to construct these piles. In figure 7 it is shown that in 15 cases voids were encountered. In six cases completely decalcsified sandstone (i.e. sand) was found. Holes were dug to the bottom of the cavities and filled with concrete.

Missing such crucial elements in a conceptual engineering-geological ground model causes delays and increases costs. Eventually, the building was erected and is still in service today (in fact both authors lectured here).

<u>*What is the value of the information contained in the geological map?*</u>

Wherever material can be found that is interesting or was at some time interesting for society (building materials, ores, fuels, calcium-carbonate for agricultural purposes) depressions or voids (caverns, shafts, tunnels) can be expected. Geological maps might help to identify materials that are or were interesting. To identify such materials, one needs to know not only the geology of a region but the cultural history of the region as well. Only this combination helps identifying material that evoked a certain interest in the past leading to underground or surface extraction and possibly subsequent backfilling.

During a desk study phase the engineering-geologists should actively look for such information. The geological map provides general guidance about formations or stages. Based on this information formations that merit special attention should be identified. Former mining activity, mines and quarries, are often not directly indicated on a geological map. Often such mining activity is mentioned within the text of booklets accompanying geological maps. Other important sources of information that should be used in conjunction with geological maps are general topographic maps, Such maps tend to include the location of adits and former quarries.

*Footnote: Case study 2 showed the importance of knowing if mining activity occurred on a construction site. The following example shows that the age of this mining activity can be way back in time and therefore more difficult to recognise. At the foot of Valkenburg castle (city of Valkenburg, province of Limburg, the Netherlands) sound rock was expected on the basis of experience with other nearby buildings and knowledge of the geology (from the many underground workings and the geological map). Subsequently the foundations for a new building were designed for sound rock. During excavation however instead, of sound rock only crushed rock with some floaters as backfill material were encountered . Investigation showed that the site hosted a 12th century quarry that produced the building stones for the first castle on the site. After producing the rocks in the 12th century the quarry was backfilled only a few years later. Because of total lack of sound rock the concept for the foundations of the 21st century building had to be modified completely.*

**Case 3: South of Namur, foundation on limestone with karst**

*Introduction*

Mont Godinne is located on a plateau east to the river Meuse and south of Namur. At this location the construction of a large building was planned in the 1980s. The authors of this publication were involved in the site investigation, for the construction of an extension to the existing structure in 2004.

*The conceptual engineering-geological model and the geological map on which it is based*

The geological map (figure 8) shows the following features:

- The site is located on a plateau above the river Meuse. The general drainage pattern follows a steep gradient downwards to the valley.
- The site is located on limestone.
- From the map it is evident that the site is located on a syncline.
- Schist (low hydraulic conductivity) can be found beneath the limestone.
- The dotted circles indicate "lost streams" that leave the surface and continue underground.

Karst features are often found where an "impermeable" layer and a limestone layer meet at the surface. Further downwards along the contact between this "impermeable" layer and the limestone, karst does not develop further because the infiltrating water is saturated with $Ca^{2+}$ from a certain depth onwards. If a syncline is present, water will accumulate in the axis of this syncline. Because a brittle rock, like limestone, will develop most discontinuities in the fold axis, karst will develop

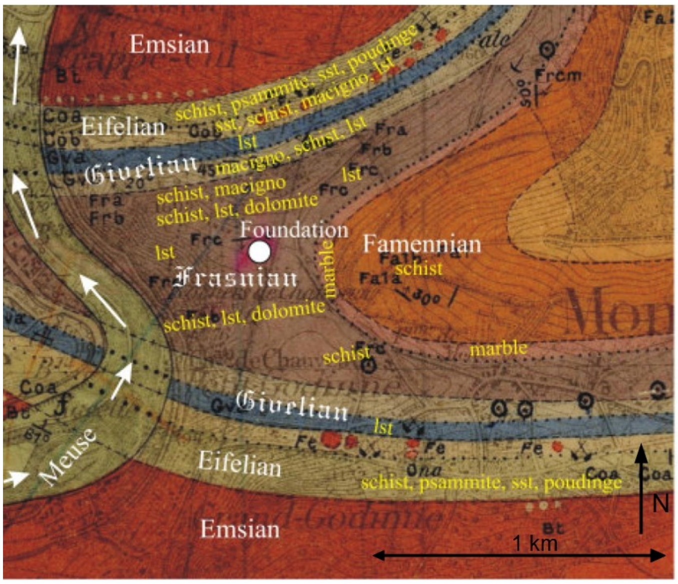


*Figure 8. Geological map of the Mont Godinne region (extract from original map: 166 Bioul-Yvoir, 1908, original scale 1:40,000; image from: Schmitz and Schroeder 2004).*

here too (figure 9). Therefore, there are two zones where karst will develop predominantly:

1) The zone where water infiltrates the ground.
2) In the axis where the limestone is most broken.

On the basis of this information provided by the geological map, the subsurface was interpreted as being composed of competent rock (limestones), with some dissolution features, overlaid by a soil cover (figure 11a). Therefore, the site investigation concentrated on determining the distance from the surface to the bedrock with a simple penetration system that consisted of hammering a rod into the ground to determine the depth to the

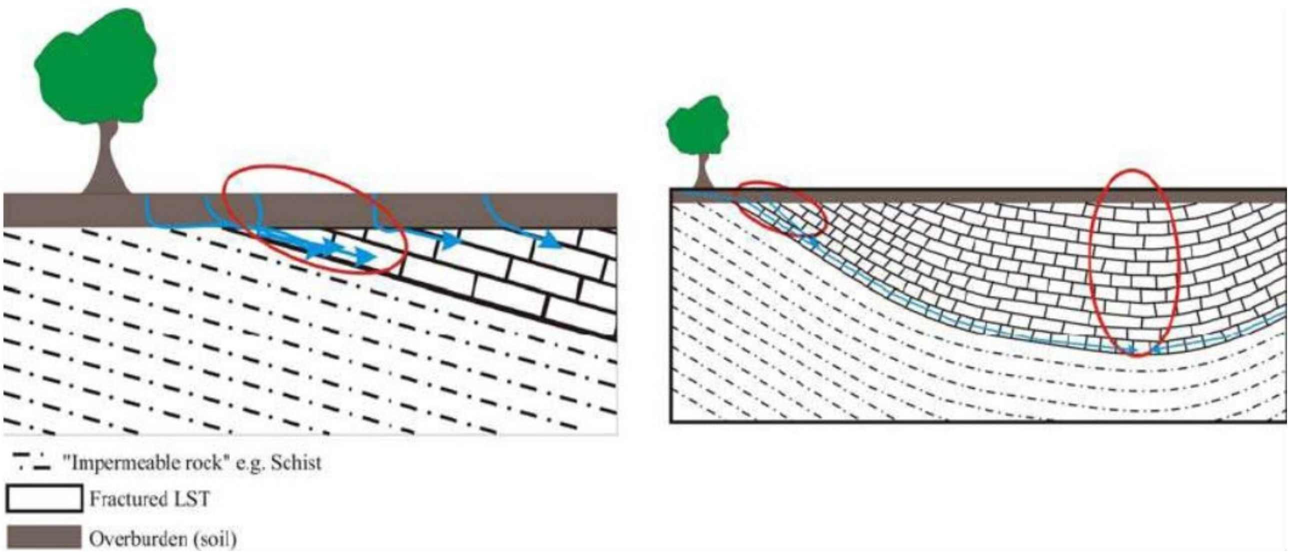


*Figure 9. Schematic overview where most karst develops. Picture from: Schmitz and Schroeder (2004).*

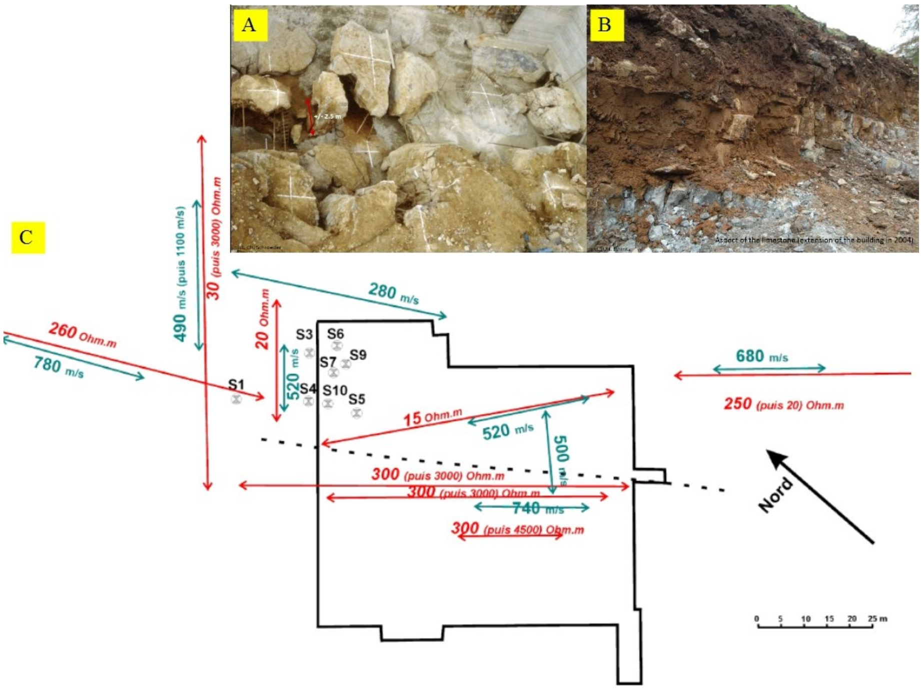


*Figure 10. A: Appearance of the bedrock after removal of the "superficial" soft clay cover. The limestone,resembles a decayed tooth instead of constituting a sound, bedrock. The smallest floating blocks were removed and the largest blocks remained in place. The ladder provides a relative scale. The crosses indicate the position of the load bearing columns in the original foundation design. B:The irregular surface of the top of the bedrock can be observed. in the excavations made for the foundation for an extension to the building in 2004. C: A geophysical survey confirmed the existence of two zones: in the west sound limestone (very high electric resistivity); in the north-east presence of clay (low resistivity).*

bedrock. Once the rod did not penetrate further into the subsurface, the top of the sound bedrock was supposed to be found.

*Risks identified on the basis of the conceptual engineering-geological model*

The engineering-geological conceptual model at that time was simple: A quasi-continuous limestone with occasionally, where the rod penetrated to larger depths, local karst holes filled with clay (figure 11a). The foundation design assumed a quasi continuous level of sound limestone and the designer selected on this basis a shallow punctual foundation. Since the geological map indicated competent rock (limestone) covered by a thin layer of soil, the site investigation consisted only of determining the depth of the limestone with a simple penetration system; that is hammering a rod into the subsurface.

*What kind of failure did occur?*

The excavation of the approximately 75 m x 75 m foundation for the building started at the south-west corner and sound limestone was encountered. However, reaching the northern corner shallow limestone was no more found. The sound bedrock was located at 8 m depth. Boreholes (S1-S10, figure 10c) were drilled to find the depth of the bedrock. The boreholes revealed discontinuous limestone blocks separated by soft clay zones or voids (figure 10a). A geophysical survey confirmed the existence of two zones (figure 10c):

- west: sound limestone (very high electric resistivity),
- north-east: presence of clay (low resistivity).

The solution that was adopted to construct the foundation consisted in manually removing the clay in the karst holes to a depth of 3 meters and by completely filling the voids completely with concrete.

*What is the value of the information contained in the geological map?*

The geological map (indirectly) contained all the information required to create a conceptual engineering-geological model that includes dissolution features of the rock as a risk for construction (figure 11b). The site where the foundation had to be made is located in one of the locations most prone to karst development: near a schist-limestone contact, in the syncline axis, well above the local major drainage system. Therefore, the correct engineering-geological model should have include the probable presence of karst in the form of channels filled with clay, floating blocks of limestone in a clay matrix, and/or voids etc. (figure 11b). Note that a differentiation according to the time the karst was formed (either Palaeokarst, Mesozoic or Cainozoic karst) helps to predict the nature of the karst more precisely as Schmitz (et al

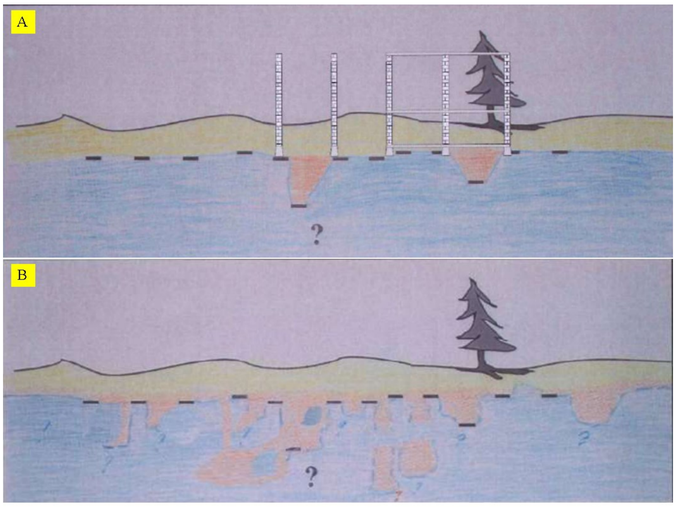


*Figure 11. Conceptual model A and B. A is the engineering geological model of limited reality assumed to be correct in the 1980s. B represents the more realistic engineering geological model.*

2007) demonstrated. Since the actual character of such karst features is difficult (impossible) to predict without further site investigation the actual morphology of these features could not have been predicted on a scale relevant to engineering on the sole basis of the geological map (see discussion in: Schmitz et al 2007). However, based on the correct conceptual model the risk of karst should have been predicted and an appropriate site investigation should have been advised (site investigation techniques in karst have been discussed by Schmitz and Schroeder 2009). Other case studies discussing engineering construction in karst in Belgium are discussed by Schmitz and Schroeder (2003), Schmitz (et al 2006) and Schmitz (et al 2007).

**Conclusion**

In this contribution we showed that on the basis of geological maps (even 100y old maps in paper form), in combination with information about the cultural history of the study area supplemented with information that can be found in books discussing the general geological history, useful conceptual engineering geological models can be made.

These models help to identify geotechnical hazards and risks. As such geological maps, on which the conceptual engineering geological model is predominantly based, help to anticipate problems in geotechnical engineering. To illustrate this, three case histories were discussed. These case histories represent different civil engineering projects in different geological settings (rock and soil with and without anthropogenic influence).

In a subsequent publication we will present more case studies and we will discuss the appropriate site investigation techniques once a conceptual engineering-geological has been made.

**References**

*Boulvain, F. (2013) Une introduction à la geologie de la Wallonie. Université de Liège.*

*Camerman, C. (1955) Le sous-sol de Bruxelles et ses anciennes carrières souterraines, Annales des travaux publics de Belgique, 2-3*

*DOV (2014) https//dov.vlaanderen.be=> Databank ondergrond Vlaanderen*

*Dreesen, R., Dusar, M. (2004) Historical building stones in the province of Limburg (NE Belgium): role of petrography in provenance and durability assessment. Materials Characterization, V. 53., pp. 273-287.*

*Eeckhout, van den, M., Poesen, J., Verstraeten, G., Vanacker, V., Moeyersons, J., Nyssen, J, van Beek, L.P.H. (2005) The effectiveness of hillshade maps and expert knowledge in mapping old deep-seated landslides. Geomorphology, V. 67, pp. 351-363*

*LNE (2014) www.lne.be/themas/bodem/grondverschuiving*

*Ost, L., Eeckhaut, van den, M., Poesen, J., Vanmaercke-Gottigny, M.C. (2003) Characteristics and spatial distribution of large landslides in the Flemish Ardennes (Belgium), Geomorph, V 47(3), pp. 329-350*

*PMW (2002) Lebendiger Stein. Naturstein aus Belgien. Pierres et Marbres de Wallonie asbl., 214 p.,V. Brancaleoni, Sprimont.*

*PMW (2012) Envie de pierres naturellement / Een natuurlijke behoefte aan steen. Pierres et* Marbres de Wallonie asbl., 23 p., Pierre Dethier, Naninne.

RVLA (2014) Geologische geschiedenis van de Vlaamse Ardennen. Regionaal landschap Vlaamse Ardennen. www.rlva.be/geologie.html

Schmitz, R.M., Schroeder, C. (2003) Line infrastructure and the role of engineering geology in the Belgian karst belt. Ingeokring Newsletter, published by the Ingenieurs-Geologische Kring (Netherlands' National Group of the International Association for Engineering Geology and the Environment. Vol. 10, N°2, 2003, pp. 10-19, (Newsletter)

Schmitz, R.M., Schroeder, C. (2004) Ingeokring (Ingenieurs-Geologische Kring: Netherlands' National Group of the International Association for Engineering Geology and the Environment) ) excursion to the Ardennes. Day II, Saturday 23 October 2004 Karst features in the Liège region, pp. 44 (Fieldwork guide)

Schmitz R.M., Viroux, S., Hick, S., Charlier, R. (2006) The role of rock mechanics in analysing overbreak: Application to the Soumagne tunnel. In: Multiphysics Coupling and Long Term Behaviour in Rock Mechanics, eds. Van Cotthem, Charlier, Thimus & Tshibangu. Balkema. Rotterdam, pp. 631-636

Schmitz, R.M., Schroeder, C., van Cotthem, A., Dethey, B. (2007) Rock engineering in karst: Belgian case histories. In: 11th Congress of the International Society for Rock Mechanics. Eds. L. Ribeiro e Sousa, C. Olalla, N. Grossmann. Taylor & Francis. Leiden. pp. 661-665 (Article in book)

Schmitz, R.M., Schroeder, C. (2009) Urban site investigation in the Belgian Karst belt. In: Culshaw, M.G., Reeves, H.J., Jefferson, I., Spink, T.W. (eds) Engineering Geology for Tomorrow's Cities. Geological Society, London, Engineering Geology Special Publications, 22, paper N° 801

Vanhulle, K. (2005) DES en Gestion des Risques Naturels 2005-2006 Présentation examen du cours instabilités de versants naturels (Prof. Ch. Schroeder)

Wal (2013) http://environnement.wallonie.be/cartosig/cartegeologique/. These maps are lithostratigraphic maps.

# ‘Building with the Subsurface’ for realizing cost-efficient infrastructure

**A.A.M. Venmans (**Deltares, P.O. Box 177, NL-2600 MH Delft, The Netherlands)

ABSTRACT: The paper introduces the concept of ‘Building with the Subsurface’ for optimising constructions to profit from subsurface conditions. The concept fits in the framework of Value Engineering. A case study for a road on soft soil illustrates the concept. Subsoil heterogeneity is expressed in sets of discrete synthetic subsoil profiles, suitable for geotechnical design calculations with conventional tools. The case study shows that the uncertainty in the whole life cost of the road ranges between ±10% and ±30%, depending on lithology and sensitivity of the construction method to subsoil uncertainty. Adding local site investigation to subsoil data from public sources reduces the uncertainty.

KEYWORDS: Subsurface model, Value Engineering, geological uncertainty, cost estimate, roads, soft soil, piled

*An earlier version of this article has been published as Venmans, A.A.M. (2013) ‘Building with the Subsurface’ for realizing cost-efficient infrastructure, Proceedings of the 18th International Conference on Soil Mechanics and Geotechnical Engineering, Paris 2013, pp 1781-1784*

## 1. BUILDING WITH THE SUBSURFACE AND VALUE ENGINEERING

Reduction of subsoil related risks was an important issue for the past few years in the Netherlands. The potential economic benefit is estimated at 1.5 % of the construction sector turnover (van Staveren 2006). However, entrepreneurs in the construction sector are easier stimulated by opportunities than by problems. Value engineering is an acknowledged method for identification of options for cost reduction. Value engineering saved between 6 and 8% of the total construction costs in U.S. highway projects in the past five years (US DoT FHWA 2011). This paper focuses on the potential of the subsurface to realize cost savings in infrastructure construction.

The lithology, engineering properties and hydrology of the subsoil determine the feasibility of construction methods and their costs. Critical parameters may concern foundation depths, the continuity of an impervious layer or geotechnical properties.

These critical parameters are often not adequately and systematically mapped in the current Dutch site investigation practice. The usual approach is based on CPT’s with typical center-to-center distances of 100 m, and soil sampling in borings even wider apart. Although this will provide a general idea of the soil profile and properties, heterogeneity will still cause substantial uncertainty. The more expensive way out is to use construction methods that are robust with respect to geological heterogeneity, such as piled embankments.

Three key elements of realizing more cost-effective infrastructure are (1) knowing the potential heterogeneity, (2) knowing its impacts on construction methods and costs and (3) reducing the impacts. This concept is called ‘Building with the Subsurface’, i.e. optimising constructions to profit from subsurface conditions. The impacts of subsurface uncertainty on construction costs are made explicit during the process. This allows informed decisions to be made on additional site investigation and finally, the selection of a construction method on the basis of costs, and uncertainty in costs. A Value Engineering / ‘Building with the Subsurface’ study can be performed in any project stage, but will be most rewarding in the feasibility stage. Usually the alignment or corridor will have been set in this stage. Choices regarding construction methods, materials and mitigation of impacts on the surrounding area are still open. The main outputs of the feasibility stage will be cost estimates, a time schedule for construction, and recommendations for mitigation of impacts.

Table 1 illustrates activities of the ‘Building with the Subsurface’ concept in the context of Value Engineering. This scheme is applied in the following virtual case study, using actual geological and geotechnical data.

## 2. EXAMPLE: FEASIBILITY STUDY OF A ROAD

### *2.1 Preparation phase*

A 2x2 lane road is to be constructed in the soft soil area around Rotterdam Airport (Figure 1). The time available for construction may be ½, 1 or 2 years, to be decided later.

The study should identify the alignment of the road running approximately north-south in the 10 km2 area, the whole life costs and their uncertainty. Whole life costs are the sum of construction costs of earthworks, drainage and pavement and costs of subsoil related maintenance. Construction methods will be selected on the basis of the 90% upper limit of their whole life cost. Also,

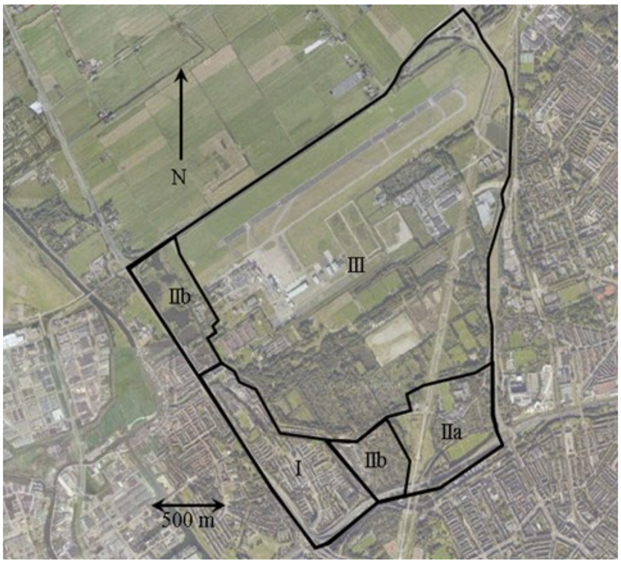


*Figure 1. Project area with subdivision according to subsoil lithology.*

the 80% confidence interval of the cost estimate should be within ±15% of the average value. 'Uncertainty' is thus expressed as the half width of the 80% confidence interval.

*2.2 Information Phase*

The elevation of the road surface will be 0.5 m above ground level. The 1:50,000 geological map indicates that the subsoil consists of 15 to 20 m of Holocene soft peat and clay over Pleistocene sands. Peat was excavated in part of the area, and artesian pressures are present in the underlying Pleistocene sands. The surface water table is at 0.6 m below ground level.

*2.3 Function Analysis Phase*

The road administrator demands that post-construction settlements should not exceed 0.15 m in 30 years, to prevent differential settlements from compromising driver comfort.
Construction should not create connections between surface water and the Pleistocene aquifer. The feasibility stage of the project will not consider relocation of utility networks.

*2.4 Creative Phase*

Two construction methods will be considered in the study: a basal reinforced piled embankment and traditional construction, using prefab vertical drains and a sand fill with temporary surcharge.

*2.5 Evaluation and Selection Phase*

The main failure mechanisms identified for the tradi-

*Table 1. Activities in a Value Engineering study, applying the 'Building with the Subsurface' concept*

| Value Engineering study | 'Building with the Subsurface' process | Acquisition of geological and geotechnical data |
|---|---|---|
| Preparation Phase | Bring together a multidisciplinary team<br>Create commitment with stakeholders and decision makers<br>Define output of the study | |
| Information Phase | Collect information on design<br>Collect geodata | Topography, general geomorphology, geology and hydrology, surface elevation |
| Function Analysis Phase | Collect and analyse data on end user specifications, impacts on the surrounding area, natural and manmade hazards | |
| Creative Phase | Prepare a longlist of construction methods and materials | |
| Evaluation and Selection Phase | Define failure mechanisms for construction methods<br>Define and assess subsoil hazards for construction methods<br>Assess feasibility of construction methods<br>Prepare a shortlist of construction methods | |
| Development Phase | Define design methods for evaluation of failure mechanisms<br>Define critical parameters of the subsurface model<br>Collect all available geological and geotechnical data<br>Synthetize sets of discrete soil profiles; define average values and uncertainty of all critical parameters<br>Perform design calculations for all soil profiles<br>Analyse the design results in terms of the output of the study<br>Optimize the design and the construction methods | *First stage*<br>Data on geology, geotechnical parameters and hydrology from public sources<br><br>*Second stage*<br>Local site investigation |
| Presentation Phase | Present the output in maps, 3D models<br>Select preferred construction methods and materials | |
| Implementation Phase | Update the list of subsoil hazards, define actions for mitigation of hazards<br>Present recommendations for later site investigation | |

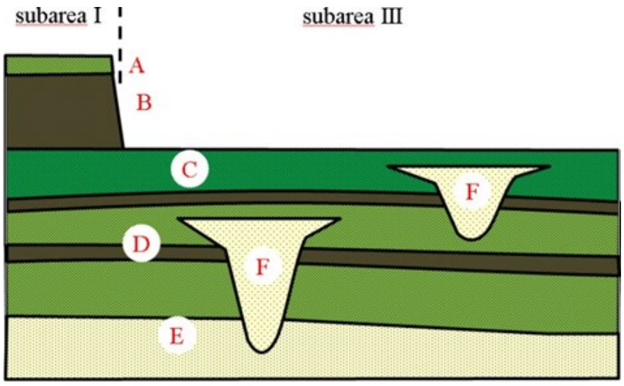


*Figure 2. Simplified geological section showing subsoil phenomena relevant to failure.*

tional construction method are: excessive post-construction settlements and differential settlements, contamination of surface water and water in the Pleistocene aquifer, damage to constructions and utility networks. Failure mechanisms for piled embankment construction include: insufficient end bearing capacity of the piles, failure of piles or load transfer platform.
Shared failure mechanisms are: instability of embankment slopes, insufficient bearing capacity of pavements and verges, and noise and vibration nuisance during construction.
A subsoil hazard is defined as the likely occurrence of a subsoil phenomenon that promotes failure. Figure 2 identifies these subsoil phenomena for the project area. This simplified geological section is redefined in terms that geotechnical engineers can understand (Baynes 2005). Table 2 lists the associated subsoil hazards. On the basis of expert judgement and local experience both

*Table 2. Subsoil hazard associated with phenomena in Figure 2*

| Unit / phenomenon | Subsoil hazard |
|---|---|
| A. Clay cover / antropogeneous deposits | Differential settlements due to old surcharges and buried sand filled channels<br>Large (post-construction) settlements |
| B. Peat | Large (post-construction) settlements |
| C. Mudflat deposits: sand, silt, clay with intermediate peat layers | Differential settlements due to buried sand filled channels<br>Large (post-construction) settlements |
| D. River deposits: sand, silt, clay with intermediate peat layers | Differential settlements due to buried sand filled channels<br>Large (post-construction) settlements |
| E. Pleistocene river deposits: sand | Artesian pressure<br>Varying bearing capacity |
| F. Buried sand filled channels | Differential settlements<br>Contact with Pleistocene deposits; artesian pressure |

construction methods were considered feasible, and included in the further process.

### 2.6 *Development Phase, first stage*

A sensitivity analysis was performed to determine which parameters have the largest contribution to the uncertainty in whole life costs of the traditional construction method. Variations of peat thickness, total thickness and unit weight of the soft layers, compression parameters and consolidation coefficient account for 95% of the variation of the costs. These critical parameters were selected for the further study.
Modelling of the lithological variation is based on 76 borings, 96 CPTs and layer boundaries of the GeoTOP 3D geological model, all obtained from the Dutch national DINO database. The information density of 10 verticals per km² is considered sufficient for compilation of a representative subsoil model, but will not allow detailed mapping of heterogeneity.
The project area is divided in 4 subareas (Figure 1), each with a different set of discrete subsoil profiles. Each profile is a synthetic stack of scenarios for the layers Pleistocene deposits, river deposits, mud flat deposits, peat and antropogeneous deposits. The total number of combinations can be huge, because up to 4 scenarios can be identified for every layer. Two hundred profiles remain for the entire project area after elimination of improbable or identical subsoil profiles. These profiles represent the subsoil variation in the area, made accessible for design calculations with conventional tools. Weighted averages and standard deviations can be determined, by estimation of the frequency of occurrence of the profiles.
Figure 3 gives an example of part of the discrete subsoil profiles synthesized for subarea I. The main difference between the areas is the peat layer that is thicker in subarea I than in subareas IIa and IIb, and has been excavated in subarea III. In subarea IIb the layer is more clayey than in subarea IIa.
Conservative estimates of the geotechnical parameters are derived from correlations with lithology and inferred volume weights. Variation coefficients of compression

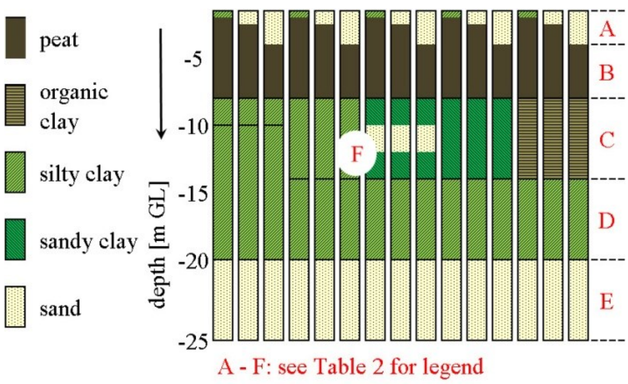


*Figure 3. Part of the synthetic soil profiles for subarea I.*

parameters are estimated at 23%; the consolidation coefficients are assumed to vary by a factor 2.
Actual CPTs are entered directly in the foundation design of the piled embankments, rather than synthetic subsoil profiles.
The analyses for the traditional method are performed in batch using the software MRoad (Venmans et al. 2005), that combines analytical settlement calculations using an isotache model with automatic determination of whole life cost. The standard deviation of the whole life costs is derived by summation of the variance caused by subsoil heterogeneity and the variance caused by permutations of the other design parameters around their average values. The variance caused by subsoil heterogeneity is reduced for length effects along the road alignment. Subsoil profiles for the soft layers are assumed to differ every 50 m. Foundation characteristics of the Pleistocene sand layer are found to vary over distances less than 20 m in the design of the piled embankment.
Settlements in the traditional method are in the order of 2.20 m in areas I and IIa, with standard deviations of 1 m. In areas IIb and III the top peat layer is much thinner or missing, and settlements are smaller, 1.40 m and 1.00 m respectively. Standard deviations are around 0.30 m. Post-construction settlements are highly variable in all subareas, with values up to 0.40 m in 30 years for the traditional method with 1 year surcharge time. However, the average values satisfy the design specification of 0.15 m. Uncertainty in compression parameters and consolidation coefficients is the main source of the uncertainty in the post-construction settlements. The post-construction settlements for a surcharge time of 2 years are smaller than the 0.15 m in all locations.
Table 3 summarizes the results of the cost calculations. The design of the piled embankment is the same for all areas, because no systematic trends can be observed in the foundation characteristics of the Pleistocene sand layer.

*Table 3. Whole life costs of 500 m road for different areas.*

| Cost parameter | I | IIa | IIb | III |
|---|---|---|---|---|
| *Traditional method, 1 year surcharge time* | | | | |
| Average | 676 k€ | 659 k€ | 612 k€ | 562 k€ |
| 90% upper limit | 815 k€ | 816 k€ | 796 k€ | 697 k€ |
| Uncertainty | 21% | 24% | 30% | 24% |
| *Traditional method, 2 year surcharge time* | | | | |
| Average | 687 k€ | 668 k€ | 588 k€ | 550 k€ |
| 90% upper limit | 762 k€ | 752 k€ | 646 k€ | 598 k€ |
| Uncertainty | 11% | 13% | 10% | 9% |
| *Basal reinforced piled embankment* | | | | |
| Average | 1601 k€ | 1601 k€ | 1601 k€ | 1601 k€ |
| 90% upper limit | 1692 k€ | 1692 k€ | 1692 k€ | 1692 k€ |
| Uncertainty | 6% | 6% | 6% | 6% |

The average whole life costs for the traditional method and their upper limits differ up to 25% between subareas. The average whole life costs for a 1 year and 2 year surcharge time are more or less equal. The 90% upper limit is much higher for the 1 year surcharge time, corresponding to 20 to 30% uncertainty. This large uncertainty is due to the large uncertainty in maintenance costs. However, the uncertainty in compression parameters and consolidation coefficients is the fundamental cause of the uncertainty in the whole life costs, since maintenance costs are related to post-construction settlements.
The whole life costs for the piled embankment are much higher than for the traditional method for this particular case. The difference mainly depends on the length of the piles and may be smaller in other cases. The uncertainty in whole life costs of the piled embankment is limited to 6% and is mainly due to uncertainty in the unit costs of construction materials.
Generally, uncertainty in the whole life costs is caused by a combination of uncertainty in the geotechnical parameters, and the sensitivity of the construction method to this uncertainty. The contribution of subsoil heterogeneity to the overall uncertainty is minor. The effects of variations between individual soil profiles or CPTs are strongly reduced by averaging along the road alignment.

### 2.7 *Presentation Phase*

The traditional method with 2 years surcharge time is the preferred construction method, based on the 90% upper limit of the whole life costs. The costs of 500 m road are visualised on a 500x500 m² grid in Figure 4. The figure also shows the location of the north-south alignment with the lowest costs. The piled embankment method will be preferred if the time available for construction is ½ year or 1 year. The traditional method with 1 year surcharge time is not eligible because of the excessive uncertainty in the costs.

### 2.8 *Local site investigation*

The project manager decides to perform an additional site investigation along the alignment shown in figure 4, aiming to reduce the uncertainty in the whole life costs of the traditional construction method with 1 year surcharge time. The site investigation is targeted at reducing the uncertainty in compression parameters and consolidation coefficient. The costs of the site investigation campaign are very modest compared to saving 1 year in construction time.

### 2.9 *Development Phase, second stage*

A new data set with CPTs, borings and laboratory data is obtained for part of area III. The center-to-center distance of the CPTs is approximately 50 m, an increase in data density by a factor 40. Soil profiles are interpreted

directly from CPT characteristics, and validated with the lithology observed in the borings. The compression constants determined in laboratory tests represent a 10% higher compressibility. The consolidation coefficients are up to 5 times higher compared to the initial parameter set. The variation coefficient of the new set of compression parameters is slightly lower at 20%; the variation in consolidation coefficients varied by a factor 2, as in the initial parameters set.
The design calculations are performed as in the earlier phases, for a surcharge time of 1 year. The settlements are 10% higher than in the initial calculations, the post-construction settlements are compatible. However, the uncertainty in the post-construction settlements was reduced from 0.17 m in the initial calculations to 0.02 m. This is caused by the significantly higher consolidation coefficients. Consolidation is completed well within the surcharge time of 1 year in all soil profiles, with only a small amount of creep compression occurring after construction. The favourable parameters also allowed a reduction of surcharge height from 2.50 m to 1.50 m, thus reducing construction cost.


*Figure 4. Whole life costs per 500x500 m² grid cell and preferred alignment of road.*

The average whole life costs for 500 m road are 523 k€, a 7% cost reduction as compared to the initial calculations for subarea III. The 90% upper limit is 560 k€, representing an uncertainty in the whole life costs of 7% only. Based on these results, the traditional construction method with 1 year surcharge time is the best option for area III.

### *3. Conclusions and recommendations*

The example shows that application of the 'Building with the Subsurface' concept in a Value Engineering study is successful. The concept can identify construction methods that fulfil all requirements, achieve cost savings, and increase the reliability of cost estimates. The method for subsoil modelling on the basis of synthetic soil profiles can successfully quantify heterogeneity using the conventional tools of geotechnical engineers.
The uncertainty in cost estimates mainly depends on uncertainty in soil parameters and the sensitivity of the construction method to these uncertainties. The cost estimate appears to depend less on lithological heterogeneity. A data density of 10 verticals/km² appears to be sufficient to reduce uncertainty in cost estimates for the traditional construction method, even though lithological heterogeneity in the Rotterdam Airport is high.
Value Engineering studies should include at least one target parameter related to the uncertainty in cost estimates, rather than focus on average cost only.
A general data set of compression and consolidation parameters should be established by systematically collecting laboratory and field observations, to reduce uncertainty in geotechnical parameters for feasibility studies.

### *References*

Baynes F.J, Fookes P.G., Kennedy J.F. 2005. The total engineering geology approach applied to railways in the Pilbara, Western Australia. *Bull Eng Geol Environ* 64: 67–94

Van Staveren M.Th. 2006. Uncertainty and ground conditions: a risk management approach. Elsevier Publishers, Oxford.

Venmans A.A.M., Förster U., Hooimeijer R.H. 2005. Integral design of motorways on soft soil on the basis of whole life costs. Proc. 16th ICSMFE Osaka. Balkema, Rotterdam

U.S. DoT Federal Highway Administration 2011. Value engineer-ing. http://www.fhwa.dot.gov/ve/

# Cargo liquefaction in bulk carriers: a review

**_Leon A. van Paassen_** *(Delft University of Technology, GeoScience & Engineering, the Netherlands)*
**_Philip J. Vardon_** *(Delft University of Technology, GeoScience & Engineering, the Netherlands)*
**_Paul Jeffrey_** *([2]Oldendorff Carriers GmbH, Lübeck, Germany )*

***Abstract***
Although liquefaction is a well-known hazard for shipping solid bulk cargoes, recent incidents in which ships capsized as a result of cargo liquefaction have triggered a debate about the regulatory guidelines. These guidelines prescribe that for some cargo types, which are typically characterised as fine grained, non-cohesive, loosely packed, wet granular materials, liquefaction may occur if the moisture content of the cargo exceeds the Transportable Moisture Limit (TML). In this paper, the results of an experimental research program in which a wide range of fine grained cargoes were characterised and tested, are presented. At the same time large international research programs were carried out by the three major iron ore producing companies. Their combined efforts were reported through the Iron Ore Technical Working Group (IOTWG) which suggested several modifications to the regulatory guidelines, resulting in higher TML values for fine grained iron ores. Comparing the outcomes of these international research programs with the experimental results presented in this paper, most conclusions were confirmed, but in some cases the results did not correspond or could be interpreted in different ways. Based on these differences, it is concluded that the suggested amendments may prove sufficiently safe for the fine grained iron ores tested by the IOTWG, but should not be generalised for all cargo types and shipping conditions. However, introducing different rules for each cargo type and shipping conditions may lead to unclear and potentially unsafe situations. Further investigations are required to improve mechanistic understanding of the processes leading to shifting cargo and ships capsizing and to improve the risk assessment approach. As these processes depend on more than just the average moisture content, such an approach should not only based on a TML alone.

***Introduction***
Cargo liquefaction is a well-known hazard for shipping solid bulk cargo. Over the last decades cargo liquefaction has caused the loss of many lives in numerous marine casualties. The most widely-known cargoes which are susceptible to liquefaction, are mineral concentrates, but also other materials such as fluorspar, certain grades of coal, pyrites, millscale or sinter/pellet feed are known to be susceptible to liquefaction. A number of recent incidents in which ships capsized while carrying wet solid bulk cargo alarmed the international society (Figure 1 and Table 1), particularly in relation to the transport of nickel ore in South East Asia. In February 2012, "The Mail on Sunday" stated that "liquefaction of nickel ore cargo was the deadliest menace to seamen around the world, causing death at an unprecedented rate.." (McGhie, 2012), after the "Vinalines Queen" capsized and sank on Christmas day, 2011. The Vietnamese bulk carrier was the fourth ship that year that sank as a result of cargo liquefaction, while transporting nickel ore

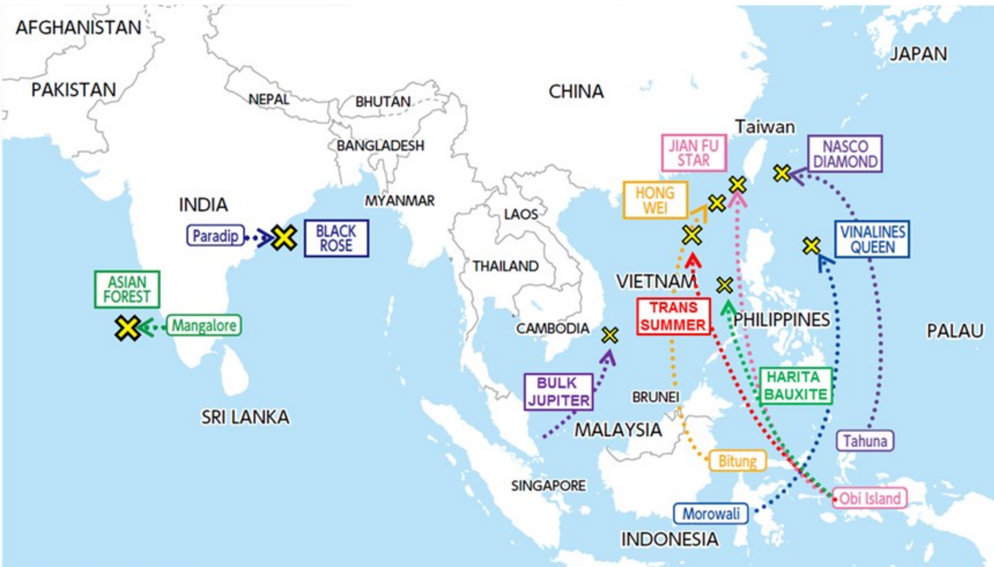


Figure 1 Sites of ships that capsized and sank caused by cargo liquefaction since 2009 (after ClassNK , 2012).

*Table 1 Ships that sank after cargo liquefaction since 2009 (after ClassNK, 2012; Mohan et al, 2010; Corbett London, 2012)*

| Date | Ship | Cargo type | Cargo weight [dwt] | Casualties |
|---|---|---|---|---|
| 9/9/2009 | Black Rose | Iron ore fines | 24,000 | 1 |
| 18/7/2009 | Asian Forest | Iron ore fines | 13,600 | 0 |
| 4/11/2010 | Nasco Diamond | Nickel ore | 56,000 | 22 |
| 27/10/2010 | Jian Fu Star | Nickel ore | 45,000 | 13 |
| 3/12/2010 | Hong Wei | Nickel ore | 50,000 | 10 |
| 25/12/2011 | Vinalines Queen | Nickel ore | 56,000 | 21 |
| 14/8/2013 | Trans Summer | Nickel ore | 56,824 | 0 |
| 17/2/2013 | Harita Bauxite | Nickel ore | 47,450 | 15 |
| 2/1/2015 | Bulk Jupiter | Bauxite | 46,400 | 18 |

from Indonesia to China, bringing the total number of crewmen that lost their life at 66. After 2012, incidents continued to occur and not only with ships carrying nickel ore. Most recently on January 2nd, 2015 the Bulk Jupiter, carrying 46,400 tons of bauxite sank 150 nautical miles off the coast of Vietnam losing all but one of its crewmen.

*Liquefaction in soils*

Liquefaction has been studied thoroughly in soil mechanics literature, mostly in relation to earthquakes. Liquefaction can typically occur in non-cohesive granular soils, which are relatively fine grained, loosely packed and saturated with water. (e.g. Boulanger and Idriss, 2006). When a load is applied on a loosely packed granular material it tends to compact. When the voids are filled completely with water, the water needs to be expelled in order to allow compaction. If the drainage capacity of the soil is limited, pore pressure, p, will increase, reducing the effective stress, σ'. The shear strength, $\tau$, , is a function of the cohesion, $c$, and friction, in which the latter depends on the effective stress and the angle of internal friction, $\varphi$. When the effective stress in a non-cohesive granular soil reduces to zero, the grains lose contact and the soil can no longer resist shear stress and starts behaving like a liquid. Fine grained, cohesive soils are considered less susceptible to liquefaction as cohesion between the grains provides shear resistance. Coarse grained soils are also less susceptible to liquefaction as the high permeability allows water to drain and prevents pore pressures to build up. The relative density of granular soils significantly affects the susceptibility for liquefaction. Densely packed granular soils are less susceptible to liquefaction, as the densely packed particles need to dilate to a looser packing in order to move. In order to dilate water needs to fill the increasing void space, which in case of limited drainage leads to a reduction in pore pressure, increasing the effective stress between the particles and consequently increasing shear strength (Figure 2). Partly saturated soils are also less susceptible to liquefaction, as the air which is present in the voids is highly compressible the increase in pore pressure will be limited.

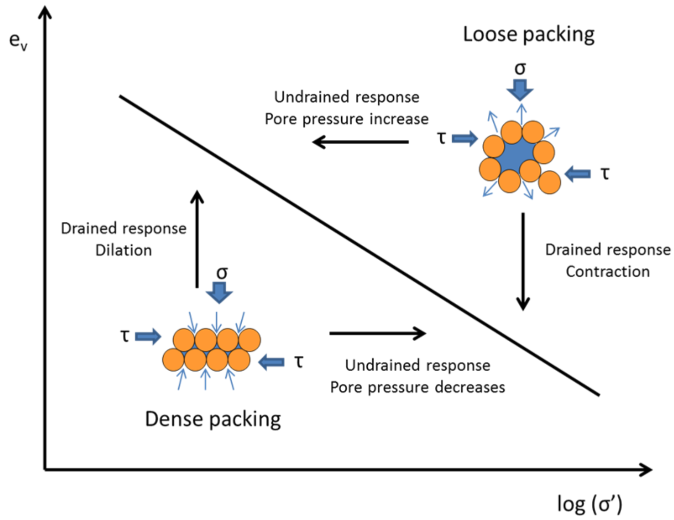


*Figure 2. Susceptibility to liquefaction is related to the relative density of a material: Loosely packed granular materials tend to contract when loaded. Undrained conditions lead to an increase in pore pressure.*

*Liquefaction in cargo*

Solid bulk cargoes are typically loosely packed granular materials. The bulk density depends on the material properties and loading conditions (grain size distribution, moisture content, drop height, cargo depth, loading rate and time between loading and shipping). When the cargo is wet during loading it might be susceptible to liquefaction. In most cases the cargo is not fully saturated with water when loaded, but it can become saturated due to compaction or drainage. Continuous loading cycles imposed by ship movements can cause the loosely packed cargo to compact. The remaining air in the void spaces between the ore grains is compressed and squeezed out, increasing the water content. When the water content approaches saturation, pore pressures may rise and induce cargo liquefaction. A rolling movement may cause the liquefied cargo to flow to one side of the ship and not completely return with a roll the other way. Progressive shift of cargo may cause the ship to list and eventually to capsize (Figure 3). Although shifting cargo is mostly attributed to liquefact ion it can also already occur before the ore is fully liquefied due to a partial loss of shear strength. Failure occurs when the stresses imposed by the cyclic load exceed the shear resistance.

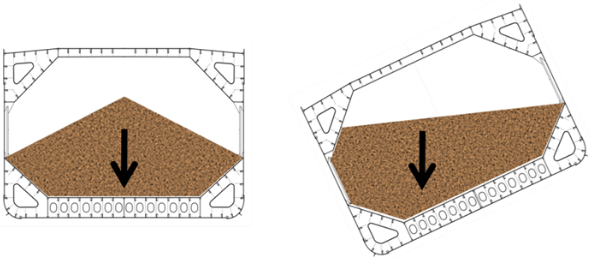

*Figure 3. Shifting cargo displaces the vertical center of gravity of a ship and can cause the ship to capsize.*

__Current cargo regulations__

The International Maritime Organisation (IMO) dealing with maritime safety, which was formally regulated after the Titanic disaster 100 years ago through the International Convention for the Safety of Life at Sea (SOLAS), provides the regulatory standards for the safe handling and transport of solid bulk cargo in the International Maritime Solid Bulk Cargoes (IMSBC) code (IMO, 2009). According to this code, solid bulk cargoes can be subdivided in three categories: Group A: Cargoes that may liquefy; Group B: Cargoes that possess a chemical hazard; and Group C: Cargoes that do not liquefy or possess a chemical hazard. The IMSBC code describes that cargoes that may liquefy contain a certain amount of small particles and some moisture. Liquefaction can occur when the average moisture content of the cargo exceeds transportable moisture limit (TML). Cargoes that contain small cohesive particles or very coarse particles are not considered susceptible to liquefaction, as in the first case the cohesion between the fine particles prevents loss of shear strength and in the second case easy drainage prevents pore pressures to build up. In some cases when the cargo is susceptible to moisture migration a liquefiable wet base may develop, or expelled water at the cargo base may harm the cargo stability even when the average moisture content of the cargo is below TML (IMO, 2009).

__Recent incidents__

Although this IMSBC code has been in existence for several decades, some incidents were reported with ships carrying fine grained iron ore from Indian ports during the monsoon season in 2009. In particular, the sinking of two merchant ships, the M.V. Asian Forest on July 17$^{th}$ and the M.V. Black Rose on September 9$^{th}$ 2009 (Figure 4), urged the Indian Ministry of Shipping to investigate the cause of events and review the existing practices and safety regulations for handling iron ore in Indian ports. They found that in both cases cargo liquefaction was the primary cause of sinking. The cargo was very wet when loaded and the movements of the ship had caused the wet cargo to liquefy and shift within the hold. The shifting cargo had caused the ships to list and eventually to capsize (Mohan et al, 2010). They found that most of the Indian iron ore is mechanically crushed after excavation and physically cleaned of impurities before being shipped overseas. It is traded as “iron ore fines”, due to its relatively fine grain size. However, at the time of the incidents the trade name “iron ore fines” was not listed in the IMSBC code. Reviewing the safety regulations they found that iron ore was categorized as a group C cargo and not considered susceptible to liquefaction. As “iron ore” was not considered liquefiable they concluded that the Indian “iron ore fines” should not be regarded as “iron ore”, but as “mineral concentrate”, which is listed as a Group A cargo, and should be handled according to the prescribed procedures for a cargo that may liquefy.

In both Indian sinking events the TML of the cargo was determined, but in the first case the required certificates were outdated and in the second case the sampling and testing methods were not performed according to the prescribed procedures. In both cases the actual moisture content had increased after the samples were taken, due

*Figure 4 The MV Black Rose capsized as a result of cargo liquefaction on 9 September 2009. This incident triggered an international debate about the safety guidelines for the transportation of fine grained iron ores (The Hindu, 2009).*

to heavy raining conditions during the storage and loading. The direct consequence of these events was that several other ships were held at bay, called back to port or forced to seek port of refuge while at sea, as certificates needed to be re-examined and tests needed to be redone. In some cases when the moisture content of the cargo turned out to be above the TML, ships were not allowed to sail, unless they unloaded their cargo or reduced its moisture content, with serious delay and significant financial consequences. Indirectly, these events caused confusion among the involved authorities about how to classify the cargo and what procedures to follow to ensure safe shipping as the boundaries between iron ore and mineral concentrate turned out to be unclear.

Despite of a long track record of safe overseas shipment, the three largest iron ore producers, Rio Tinto, BHP Billiton and Vale, realized that a lack of clarity and potential adjustments to the existing regulatory guidelines could significantly impact their trade. Proactively, they initiated large research programs, to in order to review the existing safety regulations and evaluate the prescribed procedures to ensure safe transport of liquefiable cargo. They selected a range of fine grained iron ores they produce, which had at least 10 % of dry weight particles smaller than 1 mm and at least 50 % smaller than 10 mm. For each of these ores they determined the TML using the three prescribed methods in the IMSBC code. On top of that they performed a wide range of geotechnical laboratory tests, physical model tests and numerical modelling studies and on board measurements to analyse vessel motions, sea states and vessel stability for various routes, vessel types and cargo conditions. Based on their combined research efforts they presented their conclusions and recommendations during one of the meetings of the IMO correspondence group (IOWTG, 2013a-e).

### *Experimental research program*

In parallel to these research programs, an experimental program was performed at Delft University of Technology, in which several ores were characterized and tested according to the prescribed procedures in the IMSBC code. Samples were provided by Oldendorff Carriers, a large ship-owner and world's leading dry bulk operator, based in Germany. The ores cover a wide range of fine grained ores from various ports around the world. A selection of the results of these studies is presented in this paper and compared with the outcomes of the IOTWG in order to evaluate whether their suggested amendments were justified, sufficiently conservative to prevent cargo liquefaction and also applicable for other ore types.

<u>Different types of ore</u>

Although the majority of incidents involved ships transporting nickel ore, the IOTWG focussed on fine grained iron ores, the main products of their trade. Iron ore can be defined as any naturally occurring material from which metallic iron can be extracted. The iron occurs naturally in a range of iron oxide and iron hydroxide minerals such as Magnetite ($Fe_3O_4$), Hematite ($Fe_2O_3$) and Goethite (FeOOH). Depending on the mineralogical composition the iron concentration of these ores can vary significantly. High grade iron ores, have iron concentrations exceeding 60%. They are also referred to as direct shipping ores (DSO) as they often require very little beneficiation. Low grade iron ores, such as banded iron formations (BIF), contain many other minerals and require significant 'beneficiation' to remove impurities and raise the iron ore grade to an acceptable level for blast-furnaces.

The characteristics of the cargoes provided by Oldendorff are summarized in Table 2. All the ores contained a significant amount of iron with an iron content exceeding 60%, except for the Guatemalan ore, which contained only 26% of iron. In fact the Guatemalan ore is not mined for its iron content. As it contains 2.3% of nickel it is traded as a nickel ore. The grain size distributions of the different ores ranged from poorly graded silt, sand and gravel to gap-graded crushed pellet fragments and a well-graded lateritic residual soil covering all grain sizes fine clays to remaining fragments of weathered bedrock, as shown in Figure 5. All the cargoes have much more than 10% of the dry weight particles smaller than 1 mm and more than 50% smaller than 10 mm. The parti-

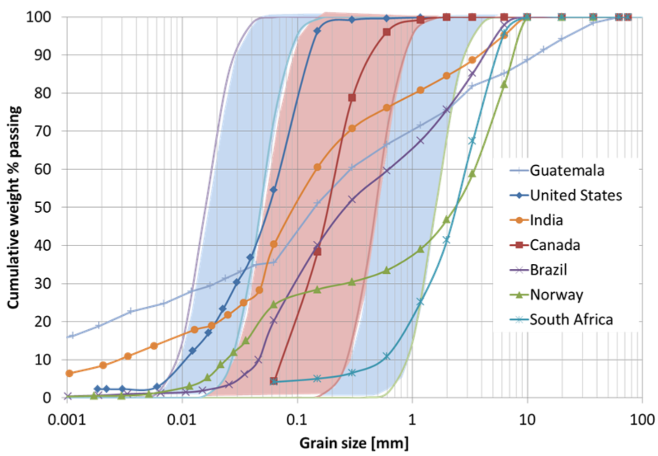


*Figure 5. Grain size distributions of the ores provided by Oldendorff.. Background colours indicate the ranges of grain size distributions which are highly susceptible to liquefaction (red) and potentially susceptible to liquefaction (blue) after Tushida (Terzaghi, 1996).*

*Table 2. Properties of the ores provided by Oldendorff.*

| Ore type[1] | <1 mm [%] | <10mm [%] | Iron content[2] [wt%] | Particle density[3] [kg/m3] | Classification (ASTM)[4] | Main minerals[5] |
|---|---|---|---|---|---|---|
| Guatemala | 70 | 89 | 26 | 4360 | well graded sandy silt with high plasticity (MH) | Quartz, Goethite, Magnetite, Lizardite |
| United States | 100 | 100 | 60 | 4850 | low plasticity silt (ML) | Hematite |
| India | 80 | 100 | 60 | 4150 | silty sand (SM) | Hematite, Goethite, Quartz |
| Brazil | 65 | 100 | 62 | 4800 | silty sand with gravel (SM) | Hematite, Goethite, Quartz |
| Canada | 99 | 100 | 63 | 4910 | silty gravel with sand (GM) | Hematite, Magnetite |
| Norway | 37 | 100 | 63 | 5070 | poorly graded sand (SP) | Hematite |
| South Africa | 20 | 100 | 62 | 4850 | well-graded gravel with sand (GW) | Hematite |

*(1) The properties of the ores are not necessarily location specific.*
*(2) Determined using X-Ray Fluorescence (XRF) Analysis*
*(3) Determined according to ASTM D5550 -06 (2006) using a gas pycnometer (Quantachrome corporation, Ultrapycnometer 1000 version 2.12)*
*(4) Classification according to ASTM D2487-11 (2011)*
*(5) Determined from X-Ray Diffraction (XRD) Analysis*

cle density of the different ores range from 4100 to 5100 kg/m$^3$, which is very high compared to the particle density  of a common sand containing minerals such as quartz, feldspar or clay minerals, which typically ranges from 2500-2700 kg/m$^3$. As a result the lithostatic stress in a layer of iron ore is often much higher than in a common sand.  The IMSBC code provides three procedures to determine the TML: the flow table test, the penetration test and the Proctor/Fagerberg test. A fourth procedure mentioned in the code is the can test. This test is not accepted as an adequate method to determine the TML. However, it is often used as an indicative test during the loading operation. The can test uses a 0.5 to 1 litre can, which is filled with a representative sample of the cargo. The can is taken in one hand and banged 25 times on a hard surface at one or two second intervals. Free moisture or fluid conditions at the surface might indicate that the cargo is susceptible to liquefaction and TML measurements are required using one of the three prescribed methods.

An important note regarding the TML is that it is expressed as a ratio between the mass of water ($m_w$) and the total mass ($m_t$). This definition is most common in mining, whereas in soil mechanics the moisture content is defined as the ratio between the mass of water ($m_w$) and the mass of solids ($m_s$). The latter is considered more convenient when calculating deformations, as the solid fraction within a specific volume remains constant while the fraction of water or gas is variable.

Flow table test

The flow table test was originally developed for Canadian mineral concentrates. It was adopted by the IMO in the 1980s and since then has been the mostly used test in industry. The test has been proven applicable for cargoes with maximum particle size of 1mm, but according to the IMSBC code it may be used up to a maximum particle size up to 7mm. It uses a standard sized conical shape mould which is placed on a standard flow table (ASTM C230-08). The mould is filled in three layers using a standard filling and tamping procedure. The tamping pressure which is applied on each layer should correspond with the stress conditions in the cargo. The total stress can be calculated from the bulk density and the height of the overburden. For example, the total vertical pressure in a layer of iron ore with a bulk density of 2000 kg/m$^3$ at a depth of 10 m is about 200 kPa. After filling and tamping, the mould is removed, leaving a truncated cone of iron ore material on the table. Next, the table is raised and dropped 50 times with a drop height of 12.5 mm at a rate of 25 drops per minute. After 50 drops a sample is taken to determine the moisture content. The tests procedure is repeated with small increments in water content. When a material is susceptible to liquefaction it starts to slump and flow when the moisture content exceeds a certain level. The increase in diameter as a result of slumping is measured. The flow moisture point is defined as the moisture content at which the cone starts slumping. The FMP is determined by measuring the average increase in cone diameter for several tests with small increments in moisture content above FMP and linearly interpolating these measurements at value of 3 mm. Below FMP the material often

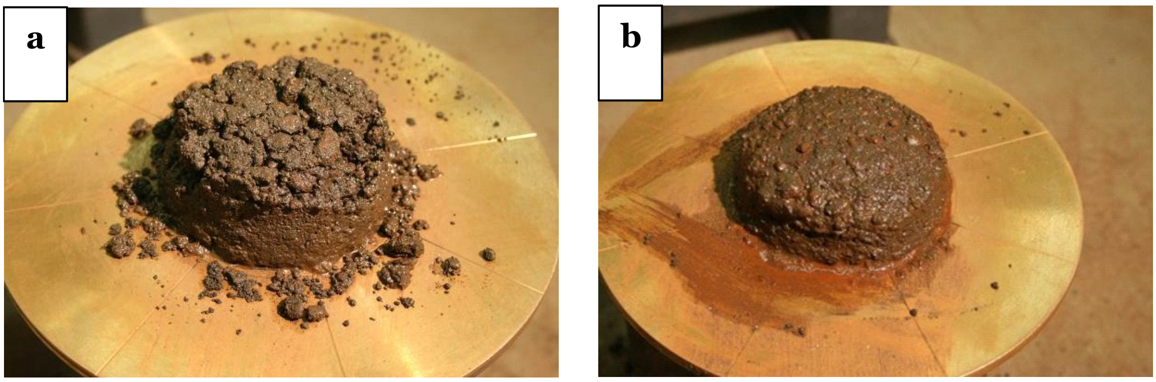


*Figure 6. An example of the flow table tests performed on the Brazilian ore a) just below and b) just above FMP.*

crumbles and bumps off in fragments with successive drops of the table. The TML is defined at 90% of FMP, to include a safety margin.

A disadvantage of the flow table tests is that it is only applicable for relatively small grain sizes. The IMBSC code states that "the test is generally suitable for materials with a maximum grain size of 1 mm and it may be applicable to materials with a maximum grain size up to 7 mm. The test is not be suitable for materials coarser than this and may also not give satisfactory results for some materials with high clay content.
The limited applicability was confirmed by the experiments as even when the largest particles exceeding 7 mm were manually removed, the FMP could only be determined for four out of seven ore types. The relatively coarse grained South African and Norwegian ores were not able to retain moisture. As they drained during the filling and tamping procedure, they fully crumbled after a few drops of the table. The Guatemalan ore did have too many coarse lumps and residual rock fragments. For the other ores it was often hard to distinguish the difference between slumping, collapse and slope failure as illustrated in Figure 6.

Penetration test

The penetration test was developed in Japan, initially to assess the TML for coal, but also considered applicable to other material types (IOTWG, 2013a). The test allows for larger grain sizes up to 25 mm, as it makes use of a larger mould. The mould is filled in four layers up to a compacted volume of about 1.7 $dm^3$. Each layer is compacted using a standard tamping procedure, in which the tamping pressure is determined similarly as in the flow table test. After tamping, the sample is put on a vibration table and a penetration bit of standard size and weight is placed on its surface. The sample is vibrated at a prescribed acceleration of 2grms [$m/s^2$] and frequency of 50 Hz for 6 minutes, after which the penetration of the bit is measured and a sample is taken to determine the moisture content. The test is repeated for small increments in moisture content (Figure 5). The Flow Moisture Point (FMP) is determined as the moisture content at which the bit reaches 50 mm penetration. Similar to the flow table test, the TML is defined at 90% of the FMP to incorporate a safety margin. The results for all tests are shown in figure 7.

During the penetration test pore pressure measurements were taken to evaluate whether liquefaction actually took place. Figure 8 shows an example of two of these measurements on the Brazilian ore just below and just above the FMP. The figures show the average and the range of measured pore pressures during cyclic loading for each load cycle as illustrated in Figure 8. Below FMP (Figure 8a) the average pore pressure remained approximately zero throughout the vibration period. Above FMP (Figure 8b) the average pore pressure gradually increased to approximately 3 kPa, which is equal to the estimated overburden pressure at sensor level and means that during most of the vibration period the ore was in a liquefied state, which confirmed that the penetration of the rod was a result of cargo liquefaction

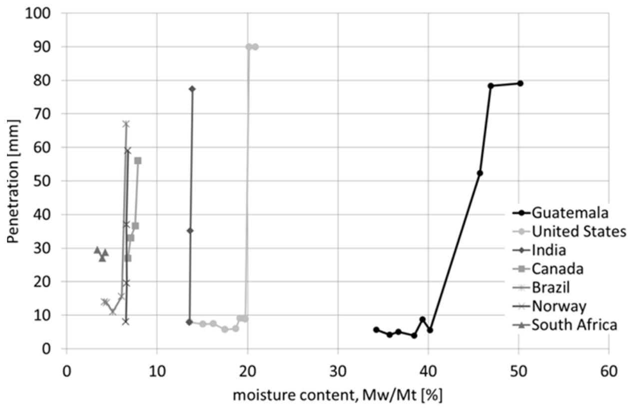


*Figure 7. Results of the penetrometer test.*

Proctor/Fagerberg Test

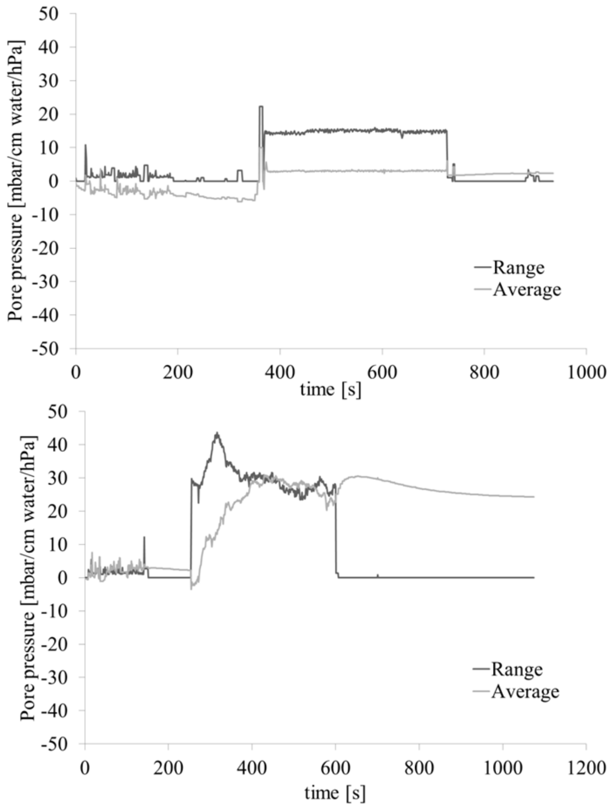


*Figure 8. Pore pressure measurements during the penetrometer test on the Brazilian ore, below the FMP (top) and above the FMP (bottom).*

The Proctor/Fagerberg test was first introduced by Proctor in the 1930s to determine the optimum moisture content (OMC) at which the maximum density could be obtained when compacting a granular material for civil engineering applications, such as subgrade for road construction. The original test procedure is described in several standards e.g. ASTM D-698-12, AASHTO T99 or JIS -A-1210:2009. The test uses a standard sized mould, which is filled in 3 to 5 layers. Each layer is compacted by dropping a standard sized hammer with a specific weight and drop height for a specific number of times on the material. After the final layer is compacted the material exceeding the upper rim of the mould is levelled off, the weight of the sample is measured to determine the bulk density and a part of the sample is dried to determine the moisture content to determine the dry density. The procedure is repeated with small increments of the moisture contents until a full compaction curve is obtained. From the curve, the maximum dry density and optimum moisture content (OMC) can be determined. A typical compaction curve is shown in figure 9. Various modified versions of the Proctor tests were developed in which the amount of compaction energy, the size of the mould or the number of layers were varied.

Fagerberg (1965) developed a modified version of the Proctor compaction test to determine the TML for solid bulk cargoes, which became known as the Proctor/Fagerberg test and is described in the IMSBC code. He found that filling the mould in five layers and applying a compaction energy of 25 blows using a hammer of 350 g and a drop height of 20 cm was most representative for the conditions he had observed in the cargo hold, taking an appropriate safety factor into account. At the optimum moisture content Fagerberg found that the degree of saturation typically varied between 70 and 75%. Assuming that a moisture content wetter than the optimum moisture content would lead to excess pore pressures limiting further compaction in the test and comparing the resulting TML values with the values obtained from the other two tests he suggested that the moisture content at which the compacted sample was 70% saturated would be a sound definition of TML. As shown in Figure 9 the maximum density and associated optimum moisture content depend on the amount of compaction energy. More compaction energy results in a higher maximum density and a lower optimum moisture content. The density obtained with the test proposed by Fagerberg corresponded with a density obtained with a 'static' tamping pressure between 100 and 200 kPa using the tamping procedure of the flow table and penetrations test.

As the bulk and dry density and a weight-based moisture content strongly depend on the density of the solid particles, Fagerberg presented the compaction curves as a plot of void ratio, $e_v$, versus volumetric water content, $e_w$, in order to compare the compaction curves of different ore types with varying particle density. The void ratio is the ratio between the volume of voids (Vv) and the volume of solids (Vs), whereas the volumetric water content

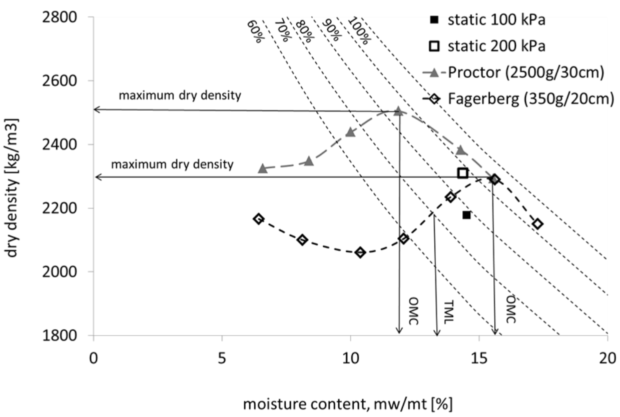


*Figure 9; Compaction curves for Indian ores using different compaction methods: the tamping procedure of the FTT and PT applying a 'static' tamping pressure of 100 and 200 kPa; the original Proctor method using a hammer weight of 2500 g and drop height of 30 cm; and the modified method suggested by Fagerberg using a hammer weight of 350 g and drop height of 20 cm as prescribed in the IMBSC code (2009), the dashed lines indicate different degrees of saturation.*

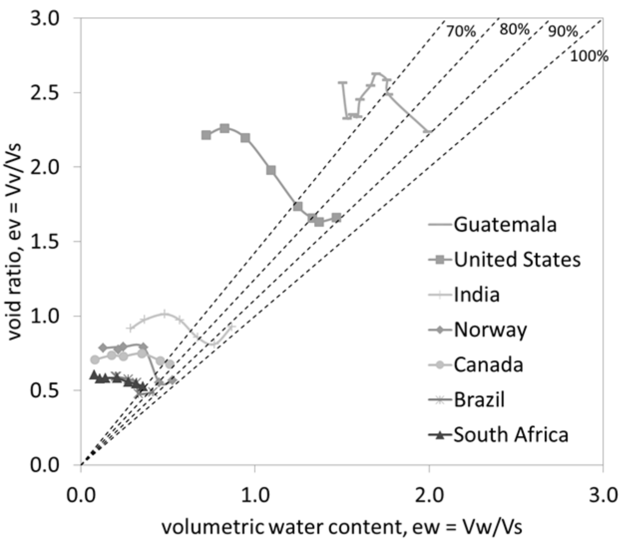


*Figure 10. Results of the Proctor/Fagerberg tests. The dashed lines indicate different degrees of saturation.*

is defined as the ratio between the volume of water (Vw) and the volume of solids (Vs). Both $e_v$ and $e_w$ can be calculated from dry density, moisture content and the particle density. The particle density is determined using a gas pycnometer e.g. according to ASTM D5550 -06 (2006).

The results of the Proctor/Fagerberg tests are shown in Figure 10 and summarized in Table 3. As can be seen in Figure 10 most curves show a decrease in void ratio with increasing moisture content towards a minimum value, which is the void ratio at maximum dry density or optimum moisture content (OMC). For some ores the OMC could not be determined. The South African and Canadian ores drained during compaction and saturation above 75% could not be obtained. Secondly these coarse grained ores showed very flat compaction curves. In contrast, the ores containing a larger fraction of fine grained particles (< 0.063 mm), showed much more compaction. The Guatemalan ore showed a very irregular pattern. With increasing moisture content the ore became very sticky. The sample could not be compacted properly as the ore squeezed away when the hammer was dropped stuck to the hammer when it was pulled up and it became impossible to avoid air inclusion when filling the mould. Air inclusions and a lower compaction energy likely resulted in lower densities than expected under a static load. Proper compaction avoiding air inclusion would probably result in higher densities or lower void ratios and lower TML values.

### *Evaluating the TML test procedures*

Comparing the different test methods shows that for all of the ores types, except for the Guatemalan ore, the different TML values are reasonably comparable (Figure 11). The absolute difference between the different tests ranges 0.7 to 2.4%, while for the Guatemalan ore the difference between the penetration test and the Proctor/Fagerberg test was 10%. For all cases, except again for the Guatemalan ore, the penetration test results in slightly lower TML than the other two tests.

The difference between the ore types is much larger than the difference between the test methods, ranging from 6.5% for the Brazilian ore to 36 or 47% for the Guatemalan ore. The TML values of the different ores can be related for a large extend to their geotechnical characteristics. In particular, various aspects of the grain size distribution are considered important characteristics affecting the susceptibility to liquefaction. This is demonstrated by: i) ores with a large amount of fines (such as the ores from India and the US and Guatemala) show significantly higher TML values than coarser grained ores (Norway and South Africa); ii) poorly graded ores, in particular the poorly graded ores with high fines content, such as the low plasticity silt from the US, have a relatively high TML value compared to well graded ores; and iii) coarse ores without fines (South Africa) are able to freely drain, easily releasing. Although the IMSBC code indicated that cohesive cargoes such as the Guatemalan ore are not susceptible to liquefaction as the cohesion between the fine particles prevents the loss of shear strength during cyclic loading, it is clear that also these cargoes lose

*Table 3 Results of the Proctor/Fagerberg tests*

| *Ore type* | *$e_w$ at TML* [Vw/Vs] [-] | *$e_v$ at TML* [Vv/Vs] [-] | *TML* [Mw/Mt] [%] | *OMC* [Mw/Mt] [%] | *Saturation at OMC* [%] |
|---|---|---|---|---|---|
| Guatemala | 1.68 | 2.60 | 36.7 | n.d. | n.d. |
| United States | 1.24 | 1.75 | 20.3 | 22 | 84 |
| India | 0.63 | 0.9 | 13.2 | 15.6 | 94 |
| Brazil | 0.33 | 0.48 | 6.5 | 6.5 | 69 |
| Norway | 0.42 | 0.61 | 7.7 | 8.5 | 85 |
| Canada | 0.48 | 0.68 | 8.8 | n.d. | n.d. |
| South Africa | 0.36 | 0.52 | 6.9 | n.d. | n.d. |

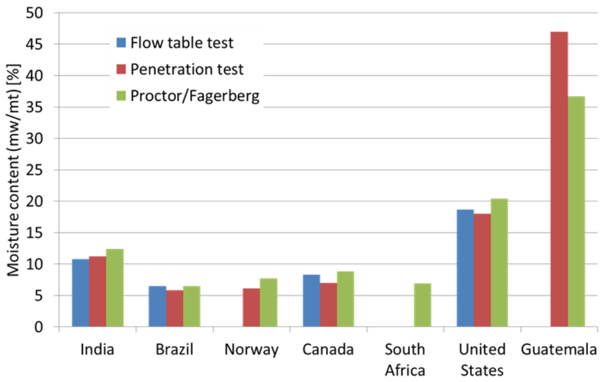


*Figure 11 Results of the three TML tests*

strength when they become too wet, considering most of the capsizing incidents involved ships transporting lateritic nickel ore.

Considering applicability not all tests were suitable for all ore types. The flow table test did not result in a TML value for the coarse grained South African and Norwegian ores as the ores drained during sample preparation and crumbled during the test instead of slumping. For the South African ore also the penetration test did not provide a TML value, as the bit didn't penetrate further than 30 mm even when the ore was fully submerged under water which seemed to indicate that for these test conditions the ore could not liquefy. The Proctor/Fagerberg test could be applied for all ore types. However, the reliability of the Proctor/Fagerberg test can be questioned as the principle of the Proctor/Fagerberg test is not based on measuring liquefaction directly, but is indirectly determined from the compaction curve. For example, according to the Proctor/Fagerberg test the South African ore has a TML of 6.9%, but according to the penetration test the relatively coarse grained iron ore cannot liquefy. Determining the TML for Guatemalan ore also turned out to be problematic. It could not be tested using the flow table test, due to the large fraction of coarse grained particles. Even when they were removed the material could not be compacted and stuck to the mould due to the cohesive and soft nature of the fine grained material. Similar problems occurred for the penetration and Proctor/Fagerberg test. The ore could not be properly compacted as with increasing moisture content the ore squeezed away under the tamper. Large air inclusions could not be avoided and lumps and remaining rock fragments were easily crushed into finer fragments during mixing and compaction. Although the code prescribes that care should be taken not to reduce grain size during mixing, it does not provide procedures how to deal with materials which are easily crushed during compaction. Consequently the TML results of the Guatemalan ore are considered unreliable.

***Results from the Iron Ore Technical Working Group***

Having tested a wide range of iron ores the IOTWG came to the conclusion that the three TML methods show significant variability and have limited applicability. They concluded that the Proctor/Fagerberg Test (PFT) is the simplest, least subjective and most precise method and therefore preferred over the other two methods (IOWTG, 2013a).

However, they also concluded that the conditions in the PFT did not correspond with actual shipping conditions. The bulk densities obtained in the PFT using the prescribed tamping procedure were significantly higher than the bulk densities measured in actual cargo and in other laboratory tests simulating shipping conditions. Using a lighter hammer of 150 g and a smaller drop height (15 cm) still resulted in higher but more representative bulk densities (IOWTG, 2013b,c). Secondly, they found that the compaction curves of the tested ores all showed an optimum moisture content (OMC) at a degree of saturation between 90 and 95%, while the mineral concentrates on which Fagerberg based the definition of TML at 70% saturation, typically had an OMC at 70-75% (IOWTG, 2013a,c).

Based on these findings they concluded that fine grained iron ore may be susceptible to liquefaction and should be listed as a separate cargo type in the IMSBC code and categorized as a group A cargo. The new cargo type named "iron ore fines" is characterized by a grain size distribution having at least 10 % of dry weight particles smaller than 1 mm and at least 50 % smaller 10 mm. The TML for "iron ore fines" should be defined using the Proctor/Fagerberg test. However, the compaction procedure of the PFT should be modified using a lighter hammer of 150 g and a lower drop height of 15 cm, to obtain bulk densities which better correspond with actual shipping conditions. Interpolating the TML at the moisture content at which the compaction curve has a degree of saturation of 80% would be sufficiently conservative.

The suggested amendments were supported by a large amount of reference tests (IOTWG, 2013d), including undrained cyclic triaxial tests, numerical modelling studies and on board measurements for various ship sizes, transport routes and cargo conditions. In all cases the resulting cyclic shear resistance exceeded the imposed cyclic stresses. Besides their evaluation of the TML test procedures they identified several other factors affecting the susceptibility to liquefaction, including ship size, moisture migration and mineralogy.

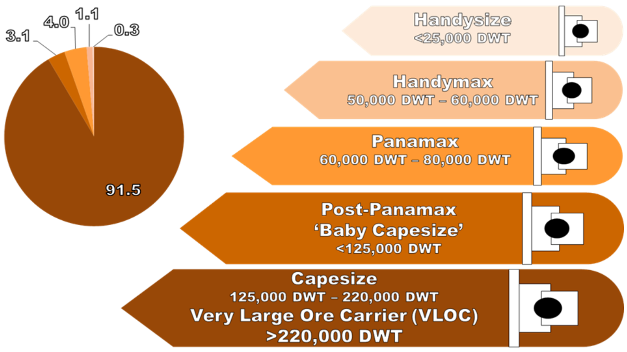


*Figure 12 Different ship sizes and the amount of total iron ore transport divided over vessel type (after Stopford, 2002; IOTWG, 2013b)*

Ship sizes have increased significantly since the prescribed test procedures have been implemented in the IMSBC code. In the early 1960s, ship size ranged from 'Handysize' with an average deadweight tonnage (dwt) of 35,000 dwt to 'Handymax' with up to 60,000 dwt. In 1965, 'Panamax' ships up to 80,000 dwt were build and in 1969 'Capesize' vessels up to 100,000 dwt appeared (Stopford, 2002). Since 2011 the largest size bulk carriers are the 'Valemax' vessels, which are specifically designed for transporting iron ores and have a loading capacity up to 400,000 dwt. Although Capesize vessels are just 10% of the global fleet of bulk carriers, they are responsible for 80% of the voyages taking 91.5% of all the iron ore for overseas transport (IOTWG, 2013b) as illustrated in Figure 12.
The probability of cargo liquefaction and consequential loss of vessel stability decreases with ship size. Firstly, Capesize vessels undergo significantly lower accelerations than Handymax or Handysize vessels. Secondly, shifting cargo in Capesize vessels results in lower listing angles (IOTWG, 2013b). This may explain why all sinking incidents listed in Table 1 involve relatively small vessels. As ship size can have a large effect on both the risk of cargo liquefaction and loss of vessel stability it should be taken into account when assessing the susceptibility to liquefaction and defining the required safety requirements.

In some Brazilian iron ores gravity drainage was observed in the cargo, causing the water to migrate downward forming a fully saturated layer at the base of the cargo. Such a wet base could cause the cargo to liquefy or induce small scale slope failure. However, based on onboard measurements and numerical analysis it was concluded that small scale instabilities which occurred in case of a wet base would not harm the stability of the vessel.

Some Australian iron ores with high goethite content showed more resistance to liquefaction and different water retention behaviour than other iron ores with low goethite content. Ores with a goethite content exceeding 35% did not liquefy during undrained cyclic triaxial tests, even when fully saturated. Consequently the IOTWG suggested that fine grained iron ores with a goethite content exceeding 35% were not susceptible to liquefaction and should therefore be considered a group C cargo.

Although the outcomes and suggested amendments by the IOTWG have not yet been accepted by the IMO, the national authorities of Australia and Brazil have approved early implementation of the suggested amendments, and ores from these countries are handled accordingly since early 2014 (Hughes, 2014).

### *Comparison of results*

The experimental results and the outcomes of the IOTWG were not in full agreement and left some issues unresolved.

The definition of iron ore fines as an iron having at least 10 % of dry weight particles smaller than 1 mm and at least 50 % smaller 10 mm seems sufficiently conservative including all the ores provided by Oldendorff of which the coarsest ore (South Africa) did not seem to be susceptible to liquefaction. However, the grain size distribution alone seems not to be sufficient to make a distinction between iron ore fines, mineral concentrates and other fine grained mineral ores containing iron such as the Guatemalan 'Nickel' Ore. As illustrated in Table 2 the properties of iron ore can vary significantly, which makes it difficult to distinguish between iron ore fines and mineral concentrate. For example some cases have been reported in which nickel ores were mixed with iron ores to increase the iron content in order to allow the material to be categorized as "iron ore" cargo and circumvent safety regulations for liquefiable cargo (Corbett London, 2014).

Comparing the results of the TML tests shows many agreements: The different tests result in different values for the TML and not applicable for all ore types. In general the Penetration Test provides lower TML values than the Proctor/Fagerberg test. The Proctor/Fagerberg test can be considered the simplest, least subjective and most precise and reproducible method. However, also the Proctor/Fagerberg test has some limitations. According to the IMSBC code the PFT is only considered suitable for cargoes with a maximum grain size smaller than 5 mm. Well graded cargoes, which full fill the defined criteria for 'iron ore fines", but also contain a significant fraction larger than 5 mm are not uncommon. Although the IMSBC does not provide methods to evaluate such cargoes, various standards exists such as ASTM D1557 (2009), which use larger moulds to accommodate for larger grain sizes. Recently, the Australian Coal Associated Research Program suggested an adjusted procedure to determine the TML for coal, using a larger mould allowing grain sizes up to 25 mm. In case, the coarsest fraction exceeds this maximum grain size, they suggested to replace this fraction by the fraction nearest to the maximum particle size of 25 mm. Another limitation of the PFT that it seems not suitable for materials that are susceptible to crushing or materials that contain a fraction of fine grained cohesive particles, such as the Guatemalan ore. This ore contained coarse fragments of weathered rock and aggregated lumps, which were easily crushed during the compaction process. Due to the cohesive nature of the fine fraction compacting the ore seemed impossible at higher moisture contents as the hammer squeezed away when the hammer was dropped and stuck to the hammer when it was pulled back up. Consequently inclusion of large air voids was difficult to avoid. The statement in the IMSBC code that clayey cargoes containing fine grained cohesive particles are not susceptible to liquefaction might be technically correct. However, increasing moisture content of cohesive materials reduces consistency and related cohesive shear strength. Consequently such cohesive cargoes can still become unstable when the cyclic load exceeds cohesive shear strength.

The suggested amendments to use a modified Proctor/Fagerberg test to determine the TML of iron ore fines is not supported by the experimental results presented in this paper. Firstly, the optimum moisture content (OMC) for the materials presented in this paper ranged from 69 to 94%. Considering that the TML should be below OMC interpreting the TML at 80 % saturation is not sufficiently conservative. Secondly, the proposition that compaction energy should be reduced, as the bulk densities in the PFT should correspond to the measured bulk densities in the cargo seems incorrect. According to the IMSBC code, the applied stress in the tamping procedure of the flow table and penetration test should correspond to the maximum expected stress level in the cargo. The bulk density obtained in the "original" Proctor/Fagerberg test corresponds to the bulk density obtained using the tamping procedure of the flow table test with a 'static' tamping pressure between 100 and 200 kPa as shown in Figure 9. These stress levels correspond to a mineral cargo depth of 5 – 10 m (IMO, 2009). When the bulk density in the cargo is relatively low for a given stress level it means the cargo is loosely packed and hence more susceptible to liquefaction (See Figure 2). Following this line of reasoning the compaction energy should be based on the expected stress conditions in the cargo instead of a corresponding bulk density.

### *Conclusions and future perspectives*

Comparing the experimental results presented in this paper and the results of the Iron Ore Technical Working Group (IOTWG) highlighted the limitations and variability in the performance of the test methods, which are prescribed to determine of the Transportable Moisture Limit for cargoes that liquefy. The results cover a wide range of cargo types, but are not in full agreement. The suggested modifications to the Proctor/Fagerberg test, which is the preferred test to determine the TML of iron ore fines, are not supported by the experimental results presented in this paper. The modifications results in higher TML values, which reduces the safety margin. Considering the members of IOTWG have a long track record of safe shipment, the safety margin may still be sufficiently conservative for the cases they considered. However, this may not be the case for other ore types or different shipping conditions, which leaves a situation where rules are not generally applicable and may lead to potentially unsafe conditions. This is recognized by the IOTWG, stating that the suggested modifications only consider iron ore fines and should not be applied for mineral concentrates, nickel ore and other group A cargoes. However, the loss of the Bulk Jupiter on the 2nd of January 2015 which was carrying bauxite – another cargo type which was not considered liquefiable - emphasizes that a more profound and generally applicable approach is required in order to better quantify the risk of shifting cargo as a result of liquefaction or other failure mechanisms. As it is shown that the risk of liquefaction depends on many factors, it is likely that such an approach includes more criteria than the TML alone.

### *Acknowledgements*

This research has been funded by Oldendorff Carriers GmbH. A vast part of the experimental work presented in this paper has been performed by students and staff from the department of Geoscience and Engineering. The manuscript has been reviewed by several colleagues. The authors would like to thank all those involved for their contribution.

### *References*

ACARP – Australian Coal Associated Research Program (2014), *Coal Transportable Moisture Limit Project TML0036 – Technical submission to the Australian Maritime Safety Authority*, Nov 2014, 24 pp

Almeida, R. (2015), Gearbulk-Owned Ore Carrier Sinks Off Vietnam, 2nd january 2015, http://gcaptain.com/gearbulk-owned-ore-carrier-sinks-vietnam/

ASTM C230/C230M-08 (2008) Standard Specification for Flow Table for Use in Tests of Hydraulic Cement, ASTM.

ASTM D698-12 (2012) Standard Test Methods for Laboratory Compaction Characteristics of Soil Using Standard Effort, ASTM.

ASTM D1557 (2009), Standard Test Methods for Laboratory Compaction Characteristics of Soil Using Modified Effort, *ASTM*.

ASTM D2487-11 (2011) Standard Practice for Classification of Soils for Engineering Purposes (Unified Soil Classification System), *ASTM*.

ASTM D5550 -06 (2006) Standard Test Method for Specific Gravity of Soil Solids by Gas Pycnometer, *ASTM*

Boulanger, R.W. and Idriss, I.M. (2006) "Liquefaction susceptibility criteria for silts and clays", *J. Geotech. Geoenviron. Eng.*, ASCE, 132(11), 1413-1426.

Chin-a-Moei, S. (2013) *BSc Thesis - Geo Engineering Report - Water Retention Research*, BSc Thesis, Geo-Engineering, Delft University of Technology.

ClassNK (2012), ClassNK's Initiatives for the Safe Carriage of Nickel Ore, ClassNK Magazine, 64th edition, December 2012, pp. 5-9.

Corbett London, A. (2014) "Intercargo warns of breach in Indonesian ore ban", *http://tradewindnews.com*, 25 July 2014, printed 12-12-2014.

Day, Robert W. (2001). *Soil Testing Manual: Procedures, Classification Data, and Sampling Practices*. New York: McGraw Hill, Inc. pp. 293–312.

Fagerberg, B., (1965a). Hazards Of Shipping Granular Ore Concentrates, *Canadian Mining Journal*, 856, July, pp 53-57.

Fagerberg, B., (1965b). Hazards Of Shipping Granular Ore Concentrates -Part II. *Canadian Mining Journal*, 856, Aug, pp 81-86.

Green, P.V. and Hughes, T.H. (1977) "Stability of bulk mineral cargoes", *Transactions of the Institution of Mining and Metallurgy, Section A: Mining Technology*, 86, A150-A158.

Hughes, J.E.M. (2014), "Iron ore fines/iron ore cargoes – early implementation of recent changes to the IMSBC code – Australia and Brazil.", *American Club Circular* No. 03/14

IMO (2009), International Maritime Solid Bulk Cargoes Code, 2009 editionand supplement, International Maritime Organization, London, 481 pp.

IOTWG (2013a-e) Iron Ore Technical Working Group Submission for Evaluation and Verification, *a) Terms of Reference; b) Marine Report; c) Iron Ore Proctor Fagerberg Test; d) Reference tests; e) Research Synopsis and Recommendations*, http://ironorefines-twg.com/, February -June 2013

JIS A 1210:2009 (2009) Test Method For Soil Compaction Using A Rammer, *Japanese Standards Association*.

Marinho, F.A.M. and Pinto, C.S. (2004) "Investigating the water retention in iron ore" *Unsaturated Soils – Volume 3, Proceedings of the 3rd international conference on unsaturated soils*, 1143 - 1146

McGhie, T. (2012, February 19), Ore can turn liquid and capsize vessels, Menace of deadly nickel cargoes in spate of sinkings, *The Mail on Sunday*.

Mohan, P.V.K., Panda, L.K., Kallam, S.A., Tamilvanan, S.P., Kumar, S.B. & Srinivas Naik, S.R. (2010), Report and recommendations of the committee on the existing practices of loading iron ore at different ports of India & cause of sinking motor vessel Black Rose and motor vessel Asian Forest off Indian Coast, reference PT-11033426/2009 PT

Stopford, M. (2009), *Maritime economics*, Routledge, London

Van de Weg, G.S. (2013), *Research to the liquefaction behavior of iron ore cargo*, MSc Thesis, Geo-Engineering, Delft University of Technology, 94pp

Paassen, LA van, Vardon, PJ, Mulder, A, Weg, G van der & Jeffrey, P (2013). Investigating the susceptibility of iron ore to liquefaction. In C Hellmich, B Pichler & D Adam (Eds.), *Poromechanics V: Proceedings of the 5th Biot Conference on Poromechanics* (pp. 1478-1487).

Terzaghi, K, Peck, RB & Mesri, G (1996), *Soil Mechanics in Engineering Practice –third editon*, John Wiley & Sons, Inc. 534 pp.

The Hindu (2009) Printable version, Jan 6, 2015 "*Oil spill could devastate orissa coast says greenpeace*", http://www.thehindu.com/news/national/other-states/ oil-spill-coulddevastate-orissa-coast-says-greenpeace/article24593.ece

# PhD abstracts from 2013

**Towards parameter limits of displacement boundary value problems for Mohr-Coulomb models (2013-01-30)**

**Author: A. Rohe**
**Promotor(s): Molenkamp, F., Van Horssen, W.T.**
**Keywords: geomechanics · boundary value problem · separation of variables · well-posedness**

To solve problems in geotechnical engineering often numerical methods such as the Finite Element Method (FEM) are used. This method can be applied for example for the calculation of the strength of dikes, the determination of the stability of (rail)road embankments, the prediction of deformations due to landfills, or the analysis of subsurface constructions such as foundations, excavation pits and tunnels.

Executing these numerical calculations frequently unreliable results are observed, which are the consequence of non-converging or unstable solutions. Indeed, often the source of the unexpected behaviour remains unknown. The present research aims to explain one of the possible causes, i.e. the influence of the applied material model on the behaviour of the numerical solution. In soil mechanics the elasto-plastic Mohr-Coulomb material model (including hardening and softening) is very commonly used.

In this research the equations of static equilibrium, on which the FEM formulation is based, are analysed and solved completely analytically. For this purpose the method of separation of variables is used, in an adapted and extended version, which allows for the solution of a larger class of problems than generally assumed. Using this method the complete analytical solution is derived for linear elasticity as well as for Mohr-Coulomb elasto-plasticity. The necessary and sufficient conditions for uniqueness and stability of the solution are determined. These conditions allow for the determination and clarification of the parameter limits for the applicability of those material models.

Using the results of this research the limits of applicability of the two considered material models can be determined for numerical applications as e.g. the Finite Element Method.

**Modelling Pile Installation Effects: A Numerical Approach (2013-06-10)**

**Author: H.K. Engin**
**Promotor(s): Van Tol, A.F.**
**Keywords: pile installation effects · finite element modelling · pile jacking**

One of the most traditional methods for supporting structures resting on soft soils is the use of piles. They generally work by transferring the loads to deeper soil layers, which can provide sufficient bearing capacity when mobilised. This type of foundations has been commonly used throughout the world and also in the western part of the Netherlands due to the typical soil profile which consists of a thick (10-20 m) soft soil layer underlain with a stiff bearing stratum composed mostly of quartz sand. In this perspective, this study sheds a light on the behaviour of piles installed in silica sand.

The bearing capacity of a pile depends on the soil properties and the stress state it is surrounded with. This is because the behaviour of granular material is governed by the packing of the grains and the contact stresses in between. The mean stress and the density can be described as the soil state, and the soil behaviour is determined on the basis of this state and the loading conditions. In the case of a displacement pile, the installation process causes a considerable amount of soil displacement and high levels of (reaction) stresses. These effects of pile installation are transmitted to soil through the interaction between sand grains and the pile, resulting in an altered soil state and properties.

A more realistic behaviour and therefore an improved design would be achieved by considering the installation effects in the analyses than performing the analysis considering a geostatic stress state around the pile(s) modelled. In current practice, the installation effects are taken into account by some empirical design methods in order to estimate the bearing capacity of foundation piles. Several field and model tests performed to investigate the influence of pile installation on the bearing capacity, have led to an evolution of the empirical models to estimate the bearing capacity of displacement piles. Recent attempts to investigate the change in the soil state were also limited either to the measurement domain (generally close to the pile) or resolution as well as the variables (e.g. displacement, strain, stress, density) that can be quantified. However, the behaviour of piles during installation, the interaction with the surrounding soil and the resulting alteration of soil properties during installation are still not well known. This information is essential, not only to make better predictions of the pile bearing capacity and its behaviour in the soil under different loading conditions, but also to be able to predict the (side) effects of pile installation on the neighbourhood.

This study is the numerical part of a larger project in which the installation effects of displacement piles are investigated both experimentally and numerically. The objective of this numerical study is to investigate the installation effects of pile jacking in sand in a numerical framework. Since the jacking operation can be considered as quasi-static loading, the dynamic effects are not considered in the analyses. For the same reason, drained conditions are assumed such that the pore pressures are only taken into account as a reduction of total stress (giving the effective stresses). As a common tool used in engineering practice, FE modelling is selected as the numerical method. In order to model pile jacking using the FEM in a standard FE code, some additional aspects have to be considered to account for the large deformation effects. In this perspective possibilities to simulate installation effects as well as the installation process were investigated and a simplified technique (the Press-Replace technique) is proposed. After a sensitivity study, the method is employed to investigate the installation effects around a jacked pile for different sand densities. In the view of the results obtained from FE simulations, the possibilities of incorporating the installation fields were investigated. Furthermore, describing the installation effects in a functional form, which allows flexibility for imposing the installation field around a so-called wished-in-place pile to model it as a jacked pile, was studied.

A novel technique is introduced to describe the installation effects of a jacked pile without simulating the penetration process. This way a jacked pile can be modelled wished-in-place and corresponding installation effects (i.e. stress, density and stiffness change) can be imposed. By the proposed method, there will be an enormous gain in term of computational effort and time in the analyses of displacement piles.

### Quantitative characterization of solute transport processes in the laboratory using electrical resistivity tomography (2013-09-18)

**Author: S. Korteland**
**Promotor(s): Heimovaara, T.J., Bruining, J.**
**Keywords: hydrogeophysics · Electrical Resistivity Tomography · inverse modelling · parameter estimation**

The shallow subsurface is an important zone from a social, economical, and environmental point of view. The increased use of the shallow subsurface together with the call for its protection and sustainable exploitation have increased the need for tools to monitor and characterize the subsurface, as well as for an improved understanding of the hydrogeological processes taking place in this zone. The limitations of traditional point sampling techniques have led to the field of hydrogeophysics, in which geophysical methods are employed to characterize the subsurface at a relatively high spatial resolution but with minimal disturbance.

A common geophysical method used for hydrogeological characterization is electrical resistivity tomography (ERT). ERT uses the injection of electrical currents and the measurement of the resulting voltages to obtain a spatial distribution of the electrical conductivity, which is related, among other things, to volumetric moisture content and ionic strength of the pore water. Although ERT is an established tool for qualitative visualization of hydrogeological processes in the subsurface, its quantitative application is relatively new and constitutes an active area of research.

The main aim of this study is to explore the quantitative characterization of solute transport processes in porous media in the laboratory using ERT. For this purpose a flexible, high-speed, and modular ERT measurement system was developed in collaboration with the Electronic and Mechanical Support Division. The new system can perform measurements with a much higher temporal resolution than commercially available field equipment. The ERT system uses a pulsed direct current source and eight channels for simultaneous voltage measurement, and can be connected to a total of 128 electrodes.

An error analysis for the ERT system shows that the measurement noise of a transfer resistance measurement (the ratio of injected current and measured voltage) in the used laboratory setup is described by a Gaussian probability distribution with $e \sim N(e*, se)$. The standard deviation of the measurement errors (se ) can be estimated from repeatability measurements, while the mean ($e*$, representing systematic errors) can be estimated from reciprocity measurements.

The ERT setup (ERT measurement system, electrodes, and experimental tank) has been used to perform a set of relatively simple, well-defined, static experiments. For these experiments the experimental tank was filled with an aqueous solution into which a solid plastic cylinder was placed. The collected ERT measurements have been used in uncoupled as well as coupled inverse approaches to estimate parameters such as the location and radius of the plastic cylinder. The statistical inversion algorithm DREAM(ZS), based on the Markov Chain Monte Carlo method, was used to estimate the model parameters. The reconstructed electrical conductivity images required in the uncoupled inversion were obtained using an algorithm based on Occam's inversion.

The model parameters estimated with the uncoupled inverse approach are corrupted due to the regularization bias introduced into the reconstructed electrical conductivity image. This bias particularly affects the estimates of the plastic cylinder's electrical conductivity and radius. The poor performance of the uncoupled inverse approach is mainly caused by the use of a smoothness prior in the image reconstruction. Obviously, such a prior is not in agreement with the sharp conductivity contrast between the plastic cylinder and the aqueous solution.

Conversely, the model parameters estimated in the coupled inverse approach are in close agreement with the measured values. The residual between the measured and simulated transfer resistances in the coupled inversion suggest that the model errors are larger than the measurement noise. The model errors are mainly attributed to errors in electrode position or shape and errors in the shape of the experimental tank. Even though the model errors are statistically significant, the total data errors are too small to significantly affect the estimated parameters values. The results show that when accurate forward models are used in a coupled inverse approach, ERT measurements can provide accurate and precise parameter estimates.

Subsequently, the feasibility of ERT to quantitatively characterize solute transport processes in our laboratory setup was explored. For this purpose, a straightforward solute transport experiment was performed, consisting of a series of three single-step tracer injections into a saturated homogeneous sand column. The use of ERT to quantify processes in porous media introduces additional uncertainty since a petrophysical relationship is required to relate the bulk electrical conductivity modelled with ERT to the properties of the porous medium. In addition, the solute transport model is subject to uncertainty in porous medium parameters as well as petrophysical parameters, uncertainty in boundary and initial conditions, and model structural errors (e.g. caused by assuming a homogeneous porous medium while in reality the medium is heterogeneous).

The reconstructed electrical conductivity images for the tracer injection experiments clearly were affected by the spatially variable resolution of the smoothness-constrained image reconstruction as well as by inversion artefacts. The applied smoothing primarily caused overestimation of the dispersion of the tracer front. The reconstructed electrical conductivities could be improved by the use of a process-based prior which includes specific information about

the solute transport process in the regularized inversion. However, the success of this prior is dependent on the accuracy of the solute transport model and petrophysical relationship used to generate the set of feasible electrical conductivity models.

The ERT measurements collected during the tracer injections were also used to estimate the parameters of a one-dimensional solute transport model in an uncoupled as well as a coupled inverse approach. In both inverse approaches, the solute transport parameters could be estimated to a high precision. Moreover, the estimated values were physically realistic and agreed relatively well with the expected values. Surprisingly, the results obtained in the

uncoupled and coupled inversions were comparable, despite the fact that the reconstructed electrical conductivities were clearly affected by regularization. An explanation for this observation was found in the variable sizes of the elements used in the ERT mesh. The smaller elements near the electrodes, where ERT spatial resolution was high, relatively contributed more to the objective function in the uncoupled inversion than the larger elements towards the centre of the domain, where ERT spatial resolution was low. As a result, the uncoupled inversion was biased towards areas with good data quality.

Although the solute transport parameters estimated with the coupled inversion are physically realistic and agree relatively well with the expected values, the (mis)fit between the observed and simulated transfer resistances suggests that significant model errors in the solute transport and/or petrophysical model must have been present. These model errors likely are the result of heterogeneities in the solute transport caused by small-scale preferential flow (cm or less). Possible causes for small-scale preferential flow are unsaturated conditions in the sand column, the periodic invasive sampling of water at the sampling ports, or non-uniform tracer injection at the sand column's bottom boundary.

Overall, the results presented in this thesis show that ERT can be used to quantitatively characterize a solute transport process in a laboratory sand column, given that a coupled inverse framework is used and the forward models are accurate enough representations of reality. In general, the success of quantitative characterization using ERT measurements is highly dependent on the information available in addition to the ERT measurements, such as information about the dominant flow and transport processes, porous medium properties, heterogeneities, and initial and boundary conditions. When little or no information is available, ERT is best used in a standard image reconstruction using a smoothness prior or other general prior. Although the resulting images will only provide qualitative information, this information could still be beneficial for the construction of an appropriate hydrogeological model. Once a hydrogeological model is constructed, its unknown parameters could be estimated using the ERT measurements in a coupled inverse approach.

In a controlled laboratory experiment additional information is readily available, which increases the feasibility of ERT for quantitative characterization. Additional information may come from imposed boundary and initial conditions and the experimental design, as well as from independent measurements of the soil's properties (e.g., porosity, water content) and petrophysical parameters. Alternatively, additional information may come from other geophysical datatypes as well as hydrological measurements.

Since the success of quantitative characterization of hydrogeological processes using ERT is highly dependent on the information available in addition to the ERT measurements, future research should focus on the integration of multiple types of geophysical data (e.g., electrical resistivity tomography, ground-penetrating radar, induced potential, self potential, electromagnetics, time-domain reflectometry) and local hydrological data (e.g., concentration, hydraulic head, flowrates).

# PhD abstracts from 2014

**Prediction of co-seismic soil slope instability with finite element methods (2014-01-09)**

**Author: L.C. Sigarán-Loría**
**Promotor(s): Kroonenberg, S.B. · Hack, H.R.G.K. · Nieuwenhuis, J.D.**
**Keywords: Earthquakes · dynamic modelling · finite elements · co-seismic displacements · predictive models**

Landslides triggered by earthquakes are complex geohazards because they comprise two independent geohazards: earthquakes and landslides. All elements and causal factors consist of (a) ground type, (b) seismic load, and (c) topographic features. In practice, hazard mapping and site-specific engineering use different approaches to simplify the assessment of earthquake-triggered landslide hazards. For instance, the pseudo-static method or the displacement-based methods. In recent years important efforts were made to improve the predictive models of co-seismic displacement by decreasing the uncertainty of their predictions.

Important limitations remain because those models do not explicitly contain the various features from the physical process (ground type + topography + seismic load). Until now, no predictive models of co-seismic displacement have been developed using numerical models (stress-strain relations embedded in connected geometrical elements), due the high cost of development and the complexities involved. In the research described in this dissertation, the finite element method (FE) was used to create a comprehensive database in which all the involved features are quantified in a simplified way, in order to constrain sources of prediction uncertainty.

In this research six generic soil types (clay and sand) were systematically modeled with a plane-strain FE. Simple step-like slopes were simulated and subjected to vertically propagating shear waves (SV-waves) until yield. The SV-waves were simulated as sinusoidal acceleration time histories. A database was subsequently created of the yield- or critical accelerations ($PHA_c$) and co-seismic displacements (u) from the slope crest. With the database, predictive models of co-seismic displacements are generated. With FE's it is possible to quantify the various parameters from all the features involved in the physical phenomenon in study. The quantified parameters pertain to (a) slope geometry (height, H, and inclination, i), (b) ground type (six soil classes, average shear wave velocity from upper 30 m, $v_{s30}$, site period, $T_s$), (c) static factor of safety (FS), and (d) the seismic load (critical acceleration, $PHA_c$, input frequency, f). Three datasets were created: magnitude-independent, soil-type dependent, and yield acceleration-dependent. On the basis of empirical relations, a hypothetical moment magnitude (M) and Arias intensity ($I_a$) were assigned to create an additional magnitude-dependent dataset.

In order to simplify the FE's formulation, a number of important assumptions were needed. Simplicity is required to constrain the amount of parameters and, therefore, sources of uncertainty. The FE's were unsaturated and used a simple linear-elastic perfectly plastic constitutive model that allows yield with a small amount of parameters. This implies that nonlinearity is not fully achieved but simplified by applying strength and stiffness increase with depth, according to the stress state. Similarly, the seismic loads used are simple artificial signals that oversimplify the real phenomena but give good insight into the interactions among the different features involved, such as: slope geometry, ground type, and basic parameters of seismic load. The main source of uncertainty from this assessment is the yield criterion, assumed conservatively ($g_{xy}$□10%) due to the lack of physical tests to validate it. The adequacy of the FE used was verified with a case study where some moderate seismic events were measured at different locations of a steep valley in Costa Rica and satisfactorily modeled.

Among the main findings, in the analysis of the multivariate qualitative relations show the possibility to constrain the dispersion of co-seismic displacement by subgrouping the datasets per soil type. The improved predictive models for the soil-dependent dataset support this finding. From the quantitative relations, it is clear that the predictive models improve considerably when using three parameters as predictors (e.g. log $PHA_c$, f, and log $v_{s30}$ or log i), compared to those that use two parameters (e.g. log $PHA_c$ and f; or log $PHA_c$ and log $v_{s30}$ or log $PHA_c$ and H). Furthermore, higher order polynomials do not improve predictive model performance. Among the derived two-predictor models, there is no improvement in using higher (third) order polynomial forms. In this case gives the use of second-order polynomials the best result, which is in agreement with the parsimony principle.

Comparisons of the outputs of the FE modelling and two simplified displacement-based methods (named "Californian" and "USGS") show smaller dispersions in the co-seismic displacements from the FE numerical models using the general magnitude-dependent and magnitude-independent datasets. For the USGS method, an empirical model was necessary to estimate the Arias intensity ($I_a$), from which fault-dependent estimations were derived. For this case, only the output resulting from reverse-oblique fault source showed a similar variability to the FE outputs and with smaller dispersion. The FE outputs provide other qualitative trends in bivariate plots sub-grouped with a second independent variable, while the other displacement-based predictive models can not provide such insight.

Furthermore, pseudo-static yield coefficients (PS-$k_y$) were estimated and compared to the assumed yield for the FE's. This showed dissimilar results. The FE yield coefficients (FE-$k_y$) are consistently larger and with higher dispersion than the PS-$k_y$. This suggests the need for calibration of the conceptual model used for yield.

This dissertation provides valuable insight into the relations among important variables comprising the main features involved in the natural phenomenon: ground

type + topography + ground motion. The findings of this research can be used as qualitative guidelines for the development of a new-generation of predictive models of co-seismic slope displacements based on numerical stress-deformation methods, for either hazard-assessment(s) or site-specific evaluation(s). Despite the simplifications imposed in the FE models to constrain sources of uncertainty in the predictive models, the results of the research show the potential for developing a new generation of predictive models of co-seismic displacement for specific datasets, for instance site-dependent or fault type-dependent predictions.
It seems worthy to explore other regression methods such as multilevel for cases when there is reversal in the direction of correlation, as found in some qualitative relations sub-grouped per soil type. The parameters used here, such as soil type and surface geometry, appear helpful to improve predictive precision. Their introduction in empirical but physically- based prediction methods is recommended therefore. The introduction of simplified seismic signals enlarged the insight too, but they are too unrealistic to modify empirical coefficients in existing prediction methods.

### Using Distributed Fiber-Optic Sensing Systems to Estimate Inflow and Reservoir Properties (2014-09-04)

**Author: F. Farshbaf Zinati**
**Promotor(s): Jansen, J.D. · Luthi, S.M.**
**Keywords: distributed pressure sensing · parameter estimation · inflow estimation · DPS · production optimization ·adjoint method · downhole monitoring · fiber optic sensors**

Recent developments in the deployment of distributed fiber-optic sensing systems in horizontal wells carry the promise to lead to a new, cheap and reliable way of monitoring production and reservoir performance. Practical applicability of distributed pressure sensing for quantitative inflow detection will strongly depend on the specifications of the sensors, details of which are currently not yet publicly available. We therefore theoretically examined the possibility to identify reservoir inflow from distributed measurements in the well. The first chapter gives a common definition of ‘smart wells’ concept, as used in hydrocarbon production. Conventional and newly-emerging well monitoring and reservoir surveillance techniques are briefly reviewed and the advantages of recent fiber-optic sensing systems are addressed. The significance of filling the gap between advanced monitoring and control technology by means of robust interpretation methods is discussed. In the second chapter a single-phase transient model for the fluid flow in the wellbore is used to investigate the time span in which dynamic phenomena in the wellbore occur. The model is based on a numerical method utilizing a flux splitting scheme and standard first-order-accurate upstream discretization is presented. Moreover the most important parameters influencing the pressure drop over a long horizontal well are investigated. The results suggested that the dynamics of the wellbore are significantly faster than the dynamics of the reservoir. Therefore in coupling a (numerical/analytical) reservoir simulator with a wellbore model, the dynamics of the wellbore can be neglected for the sake of simplicity and higher computational speed. Furthermore, the presented numerical experiments illustrated that the duration of transient-state in the wellbore was affected by the fluid compressibility. The well length, wellbore diameter and total production rate were the most important parameters to influence the total pressure-drop over the entire length of the well. The third chapter the possibility to identify reservoir inflow from distributed pressure measurements in the well is theoretically examined. The wellbore and near-wellbore are described by semi-analytical steady state models, and a gradient-based inversion method is applied to estimate the specific productivity index (SPI) as a function of along-well position. To obtain the gradients the adjoint method is used and results in a computationally very efficient inversion scheme. With the aid of two numerical experiments, the effects of well and reservoir parameters, sensor spacing, sensor resolution and measurement noise on the quality of the inversion results are investigated. The results showed that under single-phase steady-state conditions in the reservoir and the wellbore, SPIs and the associated inflow profile can be estimated from distributed pressure sensors. However, the inversion results are affected by sensor resolution, measurements noise and by the number of measurements compared to the number of unknown parameters. The negative effects of measurement noise and low sensor resolution are strongest in those areas of the well where the influx is smallest i.e. usually close to the toe. This is mainly due to the small pressure gradients along the wellbore which makes estimation of the flow rate and thus of the specific influx and of the SPI very inaccurate. The low computational time required for the proposed inversion methodology is of potential importance for applications in the real-time control of smart wells, e.g. to control coning behavior using measurements of gas or water influx. In the chapter four, the gradient-based minimization technique utilizing the adjoint method, as described in chapter three, is extended to the transient problem. Transient semi-analytical reservoir models are combined with adjoint-based minimization algorithms to estimate reservoir properties from dynamic recording of distributed pressure sensors in the well. Methods of instantaneous sink-source functions along with principle of superposition are employed to create a dynamic forward model for the coupled well-reservoir system. Analyzing measurements taken by distributed pressure sensor systems under dynamic conditions enables identifying properties of reservoir zones i.e. permeability and reservoir dimensions. By applying the proposed inversion methodology to transient pressure measurements, reservoir properties that influence the specific productivity index of each individual zone are independently estimated. In chapter five, the inversion methodology of chapter three is extended to multi-phase fluid flow condition. Resistivity measurements in addition to distributed pressure measurements are employed to estimate water and oil inflow of reservoir zones. In this approach, semi-analytical two-phase oil and water flow in the reservoir and wellbore is used to estimate two-phase specific productivity indices. Through several synthetic examples the effects of measurement noise and wellbore-reservoir geometry on the inversion results are investigated. Under steady-state conditions, the SPIs corresponding to oil and water phases and the associated oil and water inflow profiles can be estimated from distributed pressure and resistivity sensors. Combination of pressure and resistivity measurements leads to a fairly accurate estimation of the location and amount of different phases entering the wellbore from the reservoir.

### Shock-induced borehole waves in fractured formations (2014-06-11)

**Author: H. Fan**
**Promotor(s): Smeulders, D.M.J.**
Keywords: fractures · porous media · stoneley wave · attenuation · reflection · disperion · experiment

Natural or hydraulic fractures are of major importance for the productivity of hydrocarbon reservoirs. Besides fracture detection, also the aperture and extension of the fractures are essential for a correct reservoir productivity estimate. There are many ways to detect and measure fractures, such as borehole televiewers and electrical borehole scans. A practical approach to investigate fracture properties is by means of acoustic logging. In this thesis, borehole waves along fractured media are investigated theoretically and experimentally. Theoretically, the effect of a fracture intersecting a vertical borehole can be described by the introduction of a frequency-dependent (dynamic) borehole fluid compressibility which is measured in the laboratory. The dynamic fluid bulk modulus comprises the intrinsic fluid stiffness, the borehole wall distensibility, and the radial fluid seepage into the adjacent (horizontal) permeable zones. The latter two effects tend to diminish the intrinsic fluid's stiffness, giving rise to a lower effective bulk modulus amplitude and thus to a lower wave speed in the borehole. The radial oscillatory fluid seepage causes viscous friction in the adjacent zones and results in a phase lag between the pressure increase and the compression of the borehole fluid, leading to attenuation of the borehole waves. This seepage effect is expressed in terms of a so-called borehole dynamic wall impedance specifying the radial fluid velocity at the borehole wall as a function of the borehole pressure variations. If a borehole wave travels down from an undamaged zone into a fracture zone, it will encounter an impedance contrast causing the wave to partially reflect and partially transmit, thus revealing the presence of permeable fracture zone adjacent to the borehole. Stoneley wave propagation in porous and fractured formations is studied experimentally by means of a vertical shock tube facility. In this set-up, shock waves in air are generated that travel downwards into a water-saturated cylindrical rock sample that has a borehole drilled along the center axis. In this way, high-energy borehole waves can be generated with excellent repeatability. A logging probe is installed in the borehole to measure the pressure profiles. Reflection from the water-sample interface and from the free water interface can be recorded by means of a fixed pressure transducer mounted in the wall of the shock tube above the sample in the water layer. The fractures in the formation are represented by small horizontal slits in composite cylinders whose upper and lower parts are separated by small spacer poles. In this way, a variable horizontal fracture (slit) aperture can be obtained. Obviously these fractures form an open connection between the borehole fluid and the fluid outside the cylinder. Also mandrel samples are used for horizontal slits that are not open to the fluid outside the cylinder, thus representing fractures with finite radial extension. Wave experiments show that varying fracture widths significantly alter the recorded Stoneley wave pressure signal at fixed depth. The reflection and transmission of borehole tube waves over 1 and 5 mm fractures are correctly predicted by theory. Other wave experiments show that attenuation in boreholes adjacent to porous zones without fractures can be predicted by theory. This technique even allows a direct measurement of the permeability, although the acoustically measured permeability and the permeability measured by falling-head technique still show a significant discrepancy. This technique is directly applicable to fractured porous reservoir core samples.

### Soil properties from seismic intrinsic dispersion (2014-05-15)

**Author: A.S. Zhubayev**
**Promotor(s): Wapenaar, C. P. A. · Ghose, R.**
**Keywords: seismic dispersion · poroelasticity · inversion**

Theoretical and experimental studies in the past have shown the sensitivity of seismic waves to soil/rock properties, such as composition, porosity, pore fluid, and permeability. However, quantitative characterization of these properties has remained challenging. In case of unconsolidated soils, the inherently loose and heterogeneous nature complicates the task of obtaining the in situ properties and spatial variations. In this thesis, we investigate the possibility of exploiting the information of seismic intrinsic dispersion in the low frequency band (10-200 Hz), which is relevant to onshore field data, in order to quantify these physical properties, with special focus on soil porosity and permeability. In situ values of these properties are crucial in many different projects. We first investigate the frequency-dependent seismic velocity and attenuation caused by inelastic losses at grain contacts and wave-induced fluid flow at different scales (from grain size to seismic wavelength), using the theory of poroelasticity first proposed by Biot and many subsequent extensions and modifications. Several pertinent models of poroelasticity are looked at in order to find out their applicability in explaining the observed seismic dispersion. The observed dispersion can vary greatly between various unconsolidated, fully-saturated soils. Further, we develop a stress-dependent Biot (SDB) model in order to study the behaviour of seismic waves propagating through a fully-saturated porous medium subjected to different stress conditions. This is achieved by combining the mechanics of granular soils with the effective-stress laws, finally coupling with Biot's theory. Careful analyses of the underlying soil/rock physics that relate geophysical observations to the physical properties reveal an interesting feature in the property domain among several different measurements. This is an extention to some recent work done by others. We have found that it is possible to find two or more measured quantities, showing contrasting (sometimes quasi-orthogonal) behaviour in the common parameter space, such that a combination of those measured quantities leads to a physics-based uniqueness in the property estimation.
This quasi-orthogonality in the common property domain among different measured quantities is advantageously used for estimation of porosity, permeability, water saturation, and effective stress. Several numerical examples are presented where P- and S-wave velocity and attenuation are efficiently integrated in order to obtain soil properties. In addition to seismic waves, electromagnetic waves are briefly considered for

extracting extra soil properties. In this research, considerable attention has been paid to the investigation of S waves travelling through a porous medium, since S waves have well-known significance in the context of shallow subsurface characterization. Twelve selected datasets of frequency-dependent S-wave velocity and attenuation from various soft-soil sites are used in this study. Data for fully-saturated, unconsolidated soils from land/onshore environment are only considered. It is found that the behaviour of seismic intrinsic dispersion can vary greatly with the soil-type. One of the main challenges in property estimation using intrinsic dispersion relates to reliable extraction of the information of intrinsic dispersion from the recorded seismic data. The difficulty lies in the quantification of scattering attenuation, the effect of which is always present in the recorded seismograms due to the wavelength-scale and smaller heterogeneities in the subsurface. Scattering has an absorption-like effect on the transmitted seismic energy. Accordingly, determining and subtracting the scattering attenuation from the total (or apparent) attenuation is critically important. We have discussed and successfully tested an approach, achieving this goal. Several shallow vertical seismic profiling (VSP) measurements are conducted in the field using a recently developed digital, array-seismic cone penetrometer (CPT) system. CPT provides information on cone-tip resistance, sleeve friction, and pore pressure, thus offering direct, additional knowledge on geological layering, that is used to calculate the scattering attenuation. To obtain the soil properties, an inversion algorithm is presented based on simulated annealing and the poroelasticity theory. We study the sensitivity of different parameters involved in the cost function to be minimized. The most and the least sensitive parameters are discriminated based on the eigenanalyses of the covariance matrix of the gradient of the cost function. The eigenvectors and the corresponding eigenvalues of the covariance matrix are used to navigate efficiently the search algorithm in the multidimensional space and find a relatively stable, global solution of the cost function. Finally, we apply the methodology developed in this research to a VSP dataset acquired in a layered sequence of siltstone, shale and sandstone. The porous sandstone contains hydrocarbon accumulations. The influence of fluid mobility (permeability-to-viscosity ratio) on the estimated P-wave intrinsic dispersion is distinctly observed. Using optimization by simulated annealing together with VSP and well-log measurements, the Biot and squirt flow (BISQ) model is found to provide one possible mechanism for the observed dispersion. The layer-specific fluid mobility values are estimated using our approach; they are found to be close to the independent measurements of mobility using Stoneley waves and from dynamic formation-tests carried out at the same borehole. The depth distribution of fluid mobility matches well between our estimate and the independent measurements. The methodology developed and the results obtained in this research pave the way to a new direction for in situ, quantitative soil/rock characterization using seismic waves.

**Terminal Fluvial Systems in a Semi-arid Endorheic Basin, Salar de Uyuni (Bolivia) (2014-09 -30)**

**Author: J. Li**
**Promotor(s): Luthi, S.**

**Keywords: Endorheic basin · Terminal fluvial systems · Salar de Uyuni**

Many ancient sedimentary basins are interpreted as endorheic basins, internally drained basins with no direct hydrological connection to the marine environment. Some of these endorheic basins are economically important because of the abundance of hydrocarbon resources. To date, many studies have been conducted on fluvial systems in endorheic basins; however, the fluvial architecture and facies distribution in ancient fluvial systems are not fully understood. Although they are an important key to rock record interpretation, modern terminal fluvial systems in semi-arid endorheic basins are rarely reported due to difficulties such as poor accessibility. The major objectives of this study are to: (1) investigate the development in space and time of the channel morphology and sediment distribution of a distal fluvial system in a semi-arid climatic setting, and (2) to build a quantitative data set for the construction of a 3D sedimentary architecture model. The study is carried out on a river terminus system, the Río Colorado, at the edge of the world's largest salt lake, the Salar de Uyuni in Bolivia. This unconfined and largely non-vegetated river terminus provides the opportunity to acquire a large data set including field and satellite data that enables analysing the development of channel morphologies and sediment characteristics (e.g., avulsion history, splay morphology and surface dynamics). The data acquisition consists of daily precipitation data, a Global Digital Elevation Model (GDEM), a time-series Landsat imagery and high resolution WorldView-02 and QuickBird-02 satellite images, as well as surface and shallow sediment samples and high precision GPS data (Chapter 1). Changes in channel morphology of the terminal fluvial system are a function of the precipitation intensity in the catchment area (Chapter 2). The catchment area is characteristic of a mean slope of 0.0008 m/m with the highest slope near the margin and gradually decreasing slope downstream, as well as higher vegetation cover in the mountainous regions than that in the tributary delta and terminal fluvial fan. Ten peak discharge events with more than 50 m3/s have been pinpointed between 1985 and 1999. The peak discharges resulted in massive flood-out of water and sediment onto the floodplain in the very low gradient river terminus and with a cross sectional channel area of less than 80 m2. The development in space and time of crevasse splays and local avulsions was visualized by comparing Landsat MSS and TM images before and after peak discharge events. Crevasse splays expanded in peak discharge periods, and this led to amalgamation with adjacent crevasse splays by compensational stacking. The areal extent of the crevasse splays did not change in between peak discharge events. Multiple local avulsions were distinguished between 1975 and 2001. Crevasse splays and their crevasse channels can evolve over time to an entirely new river channel. Erosion greatly exceeds accretion on both banks of the river in the tributary catchment. The prominent river bank erosion is associated with an evolving channel planform such as meander morphology, channel morphology and river pattern development (Chapter 3). Normalized Difference Vegetation Index (NDVI) analysis and field investigations suggest that non-vegetation cover and abundance of desiccation cracks and burrows are the main contributors to bank erosion. Changes in channel planform are the product of continuous lateral migration and frequent overbank flooding. Shallow channels and poor development of levees in combination with in-channel accretionary benches result in frequent overbank flooding, which lead to a high density of crevasse splays over unconsolidated river banks and accretionary benches. Avulsion and chute channels together with reactivation of partially abandoned meanders and connection of headcuts and crevasse channels produce an anabranching pattern in the study area. Crevasse splays have been categorized into three classes based on their development in space and time: new crevasse splays (NCS), changing crevasse splays (CCS) and inactive crevasse splays (ICS) (Chapter 4). The occurrence of these three types of crevasse splays shows no relationship with distance along the stream. The local gradient also shows no correlation with the number of crevasse splays. By contrast, the number of crevasse splay shows an exponential increase as the cross-sectional channel area decreases. In addition, some crevasse splays are attributed to the topographic low between adjacent crevasse splays and fill in the depression by compensational stacking. The unconfined area of the system showed great variations in sediment composition downstream. The alluvial fan segment is characterized by gravel with a fining-upward sequence, whereas the upper coastal plain segment is typified by coarse sand and some fine gravel in the upstream area, gradThe work described in this thesis deals with a variety of aspects related to the storage of carbon dioxide in geological formations. In particular we focus on the transfer between the gas phase to a fluid (liquid) or solid phase. This thesis limits its interest to study the sequestration capacity of $CO_2$ in saline aquifers and more specifically on the mass transfer between $CO_2$ and the brine, show the effect of salinity and visualize the fingering of $CO_2$ rich brine in bulk phase outside a porous medium by applying Schlieren technique. Furthermore, we also illustrate the importance of shale formations in the world for storing carbon dioxide and our experimental methods to measure the sorption capacity for enhanced gas recovery- EGR. To achieve our goals we designed, constructed and improved three different setups. The main research objectives addressed in this thesis are: (1) to investigate, experimentally and numerically, the mass transfer rate of $CO_2$ to water (brine), oil (2) visualization of natural convection flow of $CO_2$ in aqueous and oleic systems, (3) to illustrate the effect of salinity on the transfer rate of $CO_2$ in bulk and porous media, (4) to model natural convection instability of $CO_2$ rich fluid flow in the bulk aqueous and oleic phase, (5) to determine the sorption capacity of shale experimentally by applying the manometric method and estimate errors based on a Monte-Carlo simulation, (6) to review shale gas formations and their potential for $CO_2$ storage. Each chapter is summarized as follows: In chapter 2, we compare numerical model results with a set of high pressure visual experiments, based on the Schlieren technique, in which we observe the effect of gravity-induced fingers when sub- and super-critical $CO_2$ at in situ pressures and temperatures is brought above the liquid, i.e., water, brine or oil. A short description of the Schlieren set-up and the transparent pressure cell is presented. The Schlieren set-up is capable of visualizing instabilities in natural convection flows in the absence of a porous medium. The experiments illustrate that natural convection currents are weakest in the highly concentrated brine and strongest in oil. Therefore, the set-up can rank aqueous salt solutions or oil in sequence of its relative importance of natural convection flows and the ensuing enhanced transfer. The experimental results are compared to numerical results. It is shown that natural convection effects are stronger in cases of high density differences. To our knowledge there are no visual data in the literature for natural convection flow of $CO_2$ in the aqueous and oleic phase in equilibrium with supercritical $CO_2$. Indeed, there is no available experiment for $CO_2$-oil. There are no data in the literature that show the presence of a diffusive boundary layer and the continuous initiation of fingers. In chapter 3 we experimentally investigated the effect of salinity and pressure on the rate of mass transfer, for aquifer storage of carbon dioxide in porous media. There is a large body of literature that numerically and studies analytically the storage capacity and the rate of transfer between the overlying $CO_2$-gas layer and the aquifer below. There is, however, a lack of experimental work that address the transfer rate into a water-saturated porous medium at in-situ conditions using carbon dioxide and brine at elevated pressures. We emphasize that the experiment uses a constant gas pressure and measures the dissolution rate using a high pressure ISCO pump. It is shown that the transfer rate is much faster than predicted by Fick's law in the absence of natural convection currents. Chapter 4 investigates the sorption of $CH_4$ and $CO_2$ in Belgian Carboniferous Shale, using a manometric set-up. Only a few measurements have been reported in the literature for highpressure gas sorption on shales. Some recent studies illustrate that, in shale, five molecules of $CO_2$ can be stored for every molecule of $CH_4$ produced. The technical feasibility of Enhanced Gas Recovery (EGR) needs to be investigated in more detail. Globally, the amount of extracted natural gas from shale has increased rapidly over the past decade. A typical shale gas reservoir combines an organic-rich deposition with extremely low matrix permeability. One important parameter in assessing the technical viability of (enhanced) production of shale gas is the sorption capacity. Our focus is on the sorption of $CH_4$ and $CO_2$. Therefore we have chosen to use the manometric method to measure the excess sorption isotherms of $CO_2$ at 318 K and of $CH_4$ at 308, 318 and 336 K and at pressures up to 105 bar. We apply an error analysis based on Monte-Carlo simulation to establish the accuracy of our experimental data. Chapter 5 reviews the global shale gas resources and discusses both the opportunities and challenges for their development. It then provides a review of the literature on opportunities to store $CO_2$ in shale, thus possibly helping to mitigate the impact of $CO_2$ emissions from the power and industrial sectors. The studies reviewed indicate that the opportunity for geologic storage of $CO_2$ in shales might be significant, but knowledge of the characteristics of the different types of gas shales found globally is required. The potential for $CO_2$ sorption as part of geologic storage in depleted shale gas reservoirs must be assessed with respect to the individual geology of each formation. Likewise, the introduction of $CO_2$ into shale for enhanced gas recovery (EGR) operations may significantly improve both reservoir performance and economics. In chapter 6 the main conclusions of the thesis are summarized. ing to fine sand downstream. Silt and clay are the dominant sediments in the lower coastal plain segment, although there is also some very fine sand. It was found that the study area is characterized by a linear decrease downstream in bedload and correspondingly an increase in suspended load deposits (Chapter 5). Thus, in the upper coastal plain bedload deposits dominate, while in the lower coastal plain suspended load deposits are prominent. A spectral library has been established for four types of surface materials using Landsat surface reflectance in combination with Landsat CDR data and field data analysis (Chapter 6). Four types of surface materials are distinguished in the river terminus: A: salty surface; B: silt-rich surface; C, clay-rich surface; D: salt. The silt-rich surface has a weak correlation with the annual precipitation while the salty surface tends to be inversely proportional to the annual precipitation. There is no relationship between the clay-rich surface and the annual precipitation. The main geomorphological changes have been identified as the formation of crevasse splays and avulsions. High annual precipitation-induced avulsions are found to lead to increased silt-rich surfaces. Channel and splay morphodynamics, longitudinal sediment dispersion pattern in the system, and surface composition in the river terminus are the focus of this study. The expected preservation potential and sequence stratigraphy of the Río Colorado system is discussed. Future work on such dryland river systems could include investigations of the mechanisms of fluvial discontinuity at the boundary between alluvial fan and upper coastal plain, the interaction between aeolian dunes and fluvial systems in the Río Colorado river system, and groundwater regimes in the coastal plain (Chapter 7).

**Mechanisms for $CO_2$ Sequestration in Geological Formations and Enhanced Gas Recovery (2014-12-17)**

**Author: R. Khosrokhavar**
**Promotor(s): Bruining, J. · Wolf, K-H.**
**Keywords: $CO_2$ sequestration · dissolution trapping · natural convection · fluid · visualization · schlieren technique ·Sorption · Shale · Monte Carlo simulation**

The work described in this thesis deals with a variety of aspects related to the storage of carbon dioxide in geological formations. In particular we focus on the transfer between the gas phase to a fluid (liquid) or solid phase. This thesis limits its interest to study the sequestration capacity of $CO_2$ in saline aquifers and more specifically on the mass transfer between $CO_2$ and the brine, show the effect of salinity and visualize the fingering of $CO_2$ rich brine in bulk phase outside a porous medium by applying Schlieren technique. Furthermore, we also illustrate the importance of shale formations in the world for storing carbon dioxide and our experimental methods to measure the sorption capacity for enhanced gas recovery- EGR. To achieve our goals we designed, constructed and improved three different setups. The main research objectives addressed in this thesis are: (1) to investigate, experimentally and numerically, the mass transfer rate of $CO_2$ to water (brine), oil (2) visualization of natural convection flow of $CO_2$ in aqueous and oleic systems, (3) to illustrate the effect of salinity on the transfer rate of $CO_2$ in bulk and porous media, (4) to model natural convection instability of $CO_2$ rich fluid flow in the bulk aqueous and oleic phase, (5) to determine the sorption capacity of shale experimentally by applying the manometric method and estimate errors based on a Monte-Carlo simulation, (6) to review shale gas formations and their potential for $CO_2$ storage. Each chapter is summarized as follows: In chapter 2, we compare numerical model results with a set of high pressure visual experiments, based on the Schlieren technique, in which we observe the effect of gravity-induced fingers when sub- and super-critical $CO_2$ at in situ pressures and temperatures is brought above the liquid, i.e., water, brine or oil. A short description of the Schlieren set-up and the transparent pressure cell is presented. The Schlieren set-up is capable of visualizing instabilities in natural convection flows in the absence of a porous medium. The experiments illustrate that natural convection currents are weakest in the highly concentrated brine and strongest in oil. Therefore, the set-up can rank aqueous salt solutions or oil in sequence of its relative importance of natural convection flows and the ensuing enhanced transfer. The experimental results are compared to numerical results. It is shown that natural convection effects are stronger in cases of high density differences. To our knowledge there are no visual data in the literature for natural convection flow of $CO_2$ in the aqueous and oleic phase in equilibrium with supercritical $CO_2$. Indeed, there is no available experiment for $CO_2$-oil. There are no data in the literature that show the presence of a diffusive boundary layer and the continuous initiation of fingers. In chapter 3 we experimentally investigated the effect of salinity and pressure on the rate of mass transfer, for aquifer storage of carbon dioxide in porous media. There is a large body of literature that numerically and studies analytically the storage capacity and the rate of transfer between the overlying $CO_2$-gas layer and the aquifer below. There is, however, a lack of experimental work that address the transfer rate into a water-saturated porous medium at in-situ conditions using carbon dioxide and brine at elevated pressures. We emphasize that the experiment uses a constant gas pressure and measures the dissolution rate using a high pressure ISCO pump. It is shown that the transfer rate is much faster than predicted by Fick's law in the absence of natural convection currents. Chapter 4 investigates the sorption of $CH_4$ and $CO_2$ in Belgian Carboniferous Shale, using a manometric set-up. Only a few measurements have been reported in the literature for highpressure gas sorption on shales. Some recent studies illustrate that, in shale, five molecules of $CO_2$ can be stored for every molecule of $CH_4$ produced. The technical feasibility of Enhanced Gas Recovery (EGR) needs to be investigated in more detail. Globally, the amount of extracted natural gas from shale has increased rapidly over the past decade. A typical shale gas reservoir combines an organic-rich deposition with extremely low matrix permeability. One important parameter in assessing the technical viability of (enhanced) production of shale gas is the sorption capacity. Our focus is on the sorption of $CH_4$ and $CO_2$. Therefore we have chosen to use the manometric method to measure the excess sorption isotherms of $CO_2$ at 318 K and of $CH_4$ at 308, 318 and 336 K and at pressures up to 105 bar. We apply an error analysis based on Monte-Carlo simulation to establish the accuracy of our experimental data. Chapter 5 reviews the global shale gas resources and discusses both the opportunities and challenges for their development. It then provides a review of the literature on opportunities to store $CO_2$ in shale, thus possibly helping to mitigate the impact of $CO_2$ emissions from the power and industrial sectors. The studies reviewed indicate that the opportunity for geologic storage of $CO_2$ in shales might be significant, but knowledge of the characteristics of the different types of gas shales found globally is required.

different types of gas shales found globally is required. The potential for CO2 sorption as part of geologic storage in depleted shale gas reservoirs must be assessed with respect to the individual geology of each formation. Likewise, the introduction of CO2 into shale for enhanced gas recovery (EGR) operations may significantly improve both reservoir performance and economics. In chapter 6 the main conclusions of the thesis are summarized.

**Combustion for Enhanced Recovery of Light Oil at Medium Pressures (2014-07-03)**

**Author: N. Khoshnevis Gargar**
**Promotor(s): Bruining, J. · Marchesin, D.**
**Keywords: air injection · light oil recovery · in situ combustion · vaporization · porous media · medium temperature oxidation · medium pressure**

Using conventional production methods, recovery percentages from oil reservoirs range from 5% for difficult oil to 50% for light oil in highly permeable homogeneous reservoirs. To increase the oil recovery factor, enhanced oil recovery (EOR) methods are used. We distinguish EOR that uses chemical methods, (partially) miscible methods and thermal methods. Air injection is categorized as a thermal recovery method as it leads to combustion and therefore high temperature in the reservoir. However, many oil recovery mechanisms are involved in air injection process, including sweeping by flue gases, field re-pressurization by the injected gas, oil swelling, oil viscosity reduction, stripping off light components in the oil by flue gas and thermal effects generated by the oxidation reactions. Our interest is in recovering light oil from low permeability heterogeneous reservoirs using air injection leading to oil combustion, as the heated oil vaporizes away from the lower permeability parts to be collected in the higher permeability streaks. Due to simultaneous vaporization, the combustion at medium pressures, i.e., at medium depth, occurs at medium temperatures. Our focus is on air injection at medium pressures (~ 10–90 bars) to reduce the high compression costs and to avoid fracturing at shallower depth. We study this process at low air injection rates to mimic the processes in the main reaction zone (away from the injection well) in an oil reservoir, which provides a long residence time for the oxygen to be in contact with the oil. The main recovery mechanism that we consider for medium pressures is the interaction between vaporization and combustion of light oil. In the thesis, we consider exclusively modeling and simulation of air injection in light oil leading to medium temperature oxidation (MTO). In MTO, all physical processes, reaction, vaporization, condensation and filtration, are active. The main purpose of the thesis is to elucidate the prevailing mechanisms in MTO. Therefore we developed a 1-D model considering light oil recovery through displacement by air at medium pressures and low injection rates and performed both numerical and laboratory experiments to validate the MTO concept. The presence of liquid fuel, which is mobile and can vaporize or condense, is a challenge for modeling of the combustion process. We only consider the one dimensional flow problem, expecting that its solution contributes to understanding the MTO process and determine the displacement efficiency. The detailed mechanism depends on diffusive processes (capillary, molecular diffusion and heat conductivity), oil composition, air injection rate, pressure, and the presence of reaction water and initial water saturation. Each chapter is summarized as follows: In Chapter 2, the modeling and simulation of the MTO process are exclusively studied including mass-, thermal and capillary-diffusion for air injection in light oil reservoirs. In this case, we consider only single pseudo-component oil, e.g., heptane as liquid fuel in dry porous rock, to improve the understanding of the oxidation/vaporization/condensation mechanisms. It turns out that the oxidation, vaporization and condensation often occur close to each other and move with the same speed in the porous medium (resonant structure). The temperature variation is bounded by the oil boiling temperature and thus not very large. We analyze the effect of capillary pressure, heat conductivity and diffusion and compare the results with the analytical solution in the absence of diffusion processes. The numerical simulation results and the analytical results with zero diffusion processes show qualitatively similar behavior. The solution consists of three types of waves, i.e., a thermal wave, an MTO wave and saturation waves separated by constant state regions. The effect of the diffusive terms is as follows. Molecular diffusion lowers the temperature in the MTO region, but creates a small peak in the vaporization region. Capillary diffusion increases the temperature upstream of the MTO region. Higher capillary diffusion increases the recovery by gas displacement and leaves less oil for combustion. The analytical solution, without diffusive terms, and the numerical solution become qualitatively different at very high capillary diffusion coefficients. The effect of thermal diffusion smoothes the thermal wave and widens the hydrocarbon vapour region. In Chapter 3, we extended 1-D model involving a two-component oil mixture, e.g., light and medium oils as pseudo-components in dry porous rock. The light component (heptane) both vaporizes and combusts, whereas medium fraction in the oil mixture only reacts with oxygen, but its vaporization is disregarded. It was anticipated that at increasing medium oil content the nature of the combustion process would change from MTO to high temperature oxidation (HTO). The main discerning factor in the MTO combustion process is the ratio between vaporization and combustion in the low injection rate regime. It turns out that also with the two-component mixture, oxidation, vaporization and condensation often occur close to each other in the MTO wave. The character of the MTO wave changes by altering the composition of the oil. Vaporization occurs upstream of the combustion process when oil mixture is composed of a higher fraction of light component. This fact confirms previously obtained analytical and numerical solutions for one component volatile oil. The combustion front velocity is high as less oil remains behind in the combustion zone. Whereas, for a predominantly medium oil mixture (0.8 of medium component fraction in volume fraction), the vaporization moves downstream of the combustion zone in the MTO wave. As more oil stays behind in the combustion zone, the velocity of the combustion zone is slower, albeit that the temperatures are much higher. Due to high temperatures, we conjecture a transition to the HTO process in this case. To summarize, numerical calculations establish a range of parameters for the bifurcation point between MTO and HTO in a two-component oil mixture. Indeed, the bifurcation point is mainly determined by the fraction of the non-volatile component. At the bifurcation the character of the combustion process changes from a vaporization-dominated (MTO) to a combustion-dominated process (HTO). In Chapter 4, we investigate the effects of water on the oxidation/vaporization/ condensation mechanisms in the MTO wave by considering a simple three phase model involving a one-component oil (e.g., heptane, pentane or dodecane) and water in porous rock. The single pseudo-component oil vaporizes/condenses as well as combusts, whereas water only vaporizes and condenses. It was anticipated that only if the boiling point of oil is around or modestly higher (below 200oC) than the boiling point of water, the presence of water is conducive to higher and faster oil recovery. The main emphasis of this Chapter is to investigate the relative importance of steam condensation, vaporization/ condensation of oil and combustion in the low injection rate regime. The numerical solution consists of a thermal wave, a steam condensation front coinciding with or downstream of the medium temperature oxidation (MTO) wave (oil vaporization and combustion), and a three-phase saturation wave region involving oil, gas and water. Numerical calculations show that the presence of water makes the light oil recovery more efficient and faster and diminishes the adverse effect of high oil boiling points. When the boiling point of the volatile oil is about or slightly higher than the boiling point of water, the speed of the MTO wave (oil vaporization/combustion front) is equal to the speed of the steam condensation front. The volatile oil condenses at the same location as the steam, which leads to complete oil recovery. However, when the boiling point of the oil is much higher than the boiling point of water, the steam condensation front moves ahead of the MTO wave. Numerical calculations make it possible to estimate the bifurcation point (oil boiling point) at which a solution for which steam condensation and combustion occur simultaneously changes to a solution where the steam condenses downstream of the combustion zone. We show that replacing the medium boiling volatile oil by a high boiling point oil (e.g., dodecane) decreases the MTO wave speed with respect to the steam condensation front and leads to delayed recovery. In Chapter 5, a set of experiments have been designed that enables investigation of the medium pressure air injection process at low injection rate in consolidated porous media saturated with one-component oil in a ramped temperature reactor. The initial aim of the laboratory experiments was to validate various aspects considered in Chapters 2-4. The experiments were carried out to evaluate the mechanisms of the combustion reaction at different pressures and injection rates. At slower rates we expect to see details that are not visible for the experiments operating at high rates and high pressures. The most important aspect in this Chapter was to observe that an oxygen sorption step takes place at low temperatures prior to the full combustion reaction. The mechanism of initial uptake of oxygen for later release was established in this work. The sorbed oxygen bonds with hydrocarbon physically or chemically leading to complete uptake of oxygen from the injected air stream at low temperatures. At a later stage, the compound, which contains the chemically or physically adsorbed oxygen, desorbs the oxygen and further undergoes oxidation reactions to produce CO and $CO_2$. The produced liquid is hexadecane; it is not altered by an oxidation reaction because it has the same viscosity and density, which argues against chemisorption. The laboratory experiments indicate displacement efficiencies between 75–90% of the Oil Initially In Place. The amount of oil burned in the air injection process relative to the amount of oil recovered in our laboratory experiments for hexadecane increased from 2% at 10 bar to 18% at 30 bar, and again decreased to 5% at 45 bar, after which it more or less remained constant. This trend was previously obtained by the analytical results of medium temperature oxidation process. It was also shown that the oil recovery is faster at higher pressures.

# Notes for the authors

- The manuscript may be written in both Dutch or English and should be sent to the editorial board (address provided at the inside front cover).
- Authors are free in choosing the subject of their contribution with the following restraints:
  - The subject is related to engineering geology and to the specific theme of the Newsletter.
  - The manuscript is not a commercial advertisement (announcements are allowed).
- Layout
  - The article should be written in Word or similar, without any formatting or layout codes. Articles should be sent to the editorial board in digital format by e-mail (e-mail address provided at the inside of the front cover).
  - Figures, drawings, and pictures should be produced in one of the common image formats: GIF, TIFF, JPEG.
  - Figures, drawings, pictures, and tables should be submitted separately; named and numbered in a logical order according to their placement in the main text. Submissions should be preferably in digital format. The print size should be selected by considering possible reduction for the final version.
  - Each article must include the author(s) name(s), affiliations and address, and a short abstract of preferably less than 100 words.

# Advertising in the Newsletter

The Newsletter is distributed to the 160 members of the Ingeokring and several companies and institutes, active in the field of Geo-Engineering. The Newsletter offers the possibility to advertise and bring your company to readers' notice.

Advertisements, preferably in English, can be published either in black/white or in colour, A4 or A5 size. Rates are listed below:

| **Size** | **Black/white** | **Full colour** |
|---|---|---|
| A4 | €375 (2 issues) | €750 (2 issues) |
| A5 | €225 (2 issues) | €450 (2 issues) |

Advertisements should be sent to the editorial board (address provided at the inside of the front cover), preferably in high resolution digital image format (e.g. PDF, GIF, TIFF, JPEG).

www.ingeokring.nl